INVESTIGATION OF SLANTED SLOTS

BY

NICHOLAS RATAJCZYK

THESIS

Submitted in partial fulfillment of the requirements
for the degree of Master of Science in Electrical and Computer Engineering
in the Graduate College of the
University of Illinois at Urbana-Champaign, 2019

Urbana, Illinois

Adviser:

Professor Jennifer Bernhard

Abstract

With the number of wireless devices and demand for information transmitted wirelessly dramatically increasing, being able to develop simple and reliable antennas with large bandwidths is becoming more important. The size of many of these wireless devices can also be small, introducing yet another challenge for antenna designers. Some common types of antennas currently used for such applications include various forms of microstrip antennas. This thesis, however, investigates using a slanted slot to meet these design constraints. In this study, it is shown that the bandwidth of a quarter-wave slot can be enhanced by placing the slot on a slant to the edge of a metallic patch rather than placing it orthogonally to the edge. The work reported in this thesis also shows that not only does the bandwidth for a slanted slot increase, but the behavior of the slot becomes more robust to changes in the size of the metallic plate containing the slot. This same effect is studied with the analogous trapezoidal half-wavelength slot; however, while these benefits are found to still exist for the trapezoidal slot, the bandwidth does not increase as much as for the slanted slot case. The results of this study were distilled into a design procedure and the procedure was evaluated by designing a slanted slot and comparing its measurements with the simulated results. In the end it was shown that slanted slots are able to achieve larger bandwidths while also being more reliable due to their resilience to changing size constraints, all while remaining simple and easy to manufacture.

Acknowledgments

First, I would like to thank my adviser Professor Jennifer Bernhard for her constant support and guidance throughout my research. It was a great experience to be able to learn from her, and I am grateful for all of her assistance. I would also like to thank my research group as they were able to not only help provide valuable feedback on my work but also be a great group of friends. Finally, I would like to thank my friends, family, and parents for their love and encouragement. I could not have made it this far without them by my side.

Contents

Chapter 1: Introduction

With the rising number of wireless devices and the demand for large amounts of information, the need for reliable antennas that are easy to manufacture and have large bandwidths is ever increasing. The size of these devices can also vary widely and can often be small, making it more difficult for antenna designers. With these constraints it would be beneficial to have a type of antenna resilient to the space and ground plane it occupies, small, easy to design, and with as large a bandwidth as possible.

Commonly-used small antennas are various types of microstrip patch antennas (MSAs). These are very easy to make and have been made in many different shapes and configurations such as rectangles or circles or many different patterns created by cutting away portions of the edges. It is also common to see slots used with these microstrip antennas; however, the slots are usually used to direct the current flow on the microstrip patch and enhance the bandwidth of the antenna, but they do not usually play a role in radiation.

One example of this is a meander line [1]. This can be thought of as either a long path that has been snaked in order to save space, or as a rectangular patch that has many slots in the sides to force the current to follow a specific path. Another example of MSAs using slots is when they are used to create multiple metallic paths [2]. These paths are designed to be different lengths and will therefore cause the antenna to resonate at different frequencies, making it a multi-band antenna.

Not only can the slots be used to enhance an MSA, but they can be the radiator of the MSA. Slots can either be cut in the shape of a simple rectangle within a metallic plate, or they can be more complicated like a U-slot [3]. The U-slot antenna is an MSA that acts in a similar way to the meander line mentioned above where the length of the slot dictates the resonance, but the physical turning helps to improve the bandwidth.

The slots can also either be cut within the metallic plate or off the edge of the plate. As discussed in Chapter 2, a slot cut in the middle of a metallic plate will act as a half-wave resonator while a slot cut on the edge will act as a quarter-wave resonator. Being resonant antennas, both types of antenna will be resonant at frequencies dependent on the physical length of the slots, and their bandwidths are centered around these frequencies.
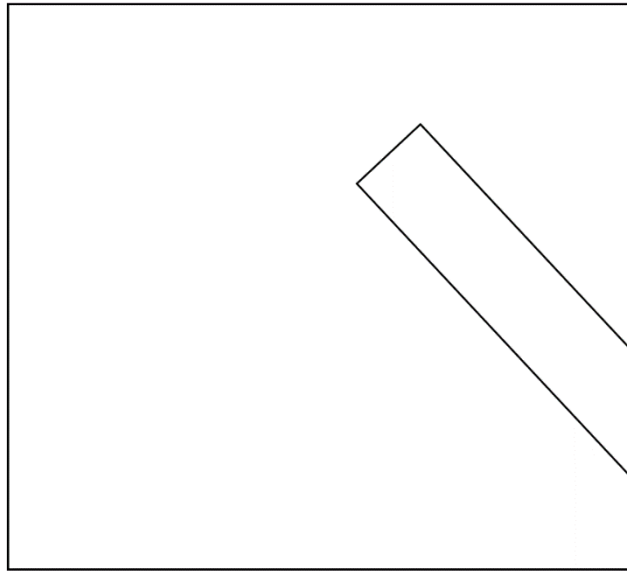
Figure 1: Basic geometrical layout for proposed slanted slot

One key difference between the slot antenna and an MSA is that, according to Babinet's principle, the slots need to be surrounded by an infinite metallic plate to perform ideally. However, an infinite plate is impossible to realize, and finite plates that are "large enough" will allow the slot to behave nearly ideally. This means that even though the size of the slot and the way it is fed impact how the slot is supposed to behave, the size of the ground plane it is contained within will also play a role in the quality and performance of the antenna. Typically, the smaller the ground plane, the worse the antenna performs. But as discussed above, many antennas can have significant limitations on the size of the overall antenna. Therefore, any way to allow the ground plane to be as small as possible while still behaving as intended is very beneficial to the use of the antenna.

Another issue posed by slot antennas and other resonant antennas is that they have narrow bandwidths. With the great demand for wirelessly-transmitted information, antenna bandwidth is extremely important. While some of the antennas previously discussed try to increase the bandwidth through meandering or bending the paths of the radiators, this thesis investigates whether the bandwidth of a quarter-wave slot antenna can be increased by placing the antenna on a slant to the edge of a metallic patch. A basic diagram of the proposed slanted slot is shown in Figure 1.

The reasoning behind this idea is that a slot antenna is a resonant structure that resonates based on its length. For a slot in the middle of a metallic plate, the slot will be resonant when it is

excited at a frequency where the length of the slot is about one half-wavelength. Similarly, a slot can be cut off the edge of the plate; however, this slot will be resonant when excited at a frequency where the length of the slot is one quarter-wavelength. But by placing this edge slot on a slant, one side becomes longer than the other. The hypothesis is that this difference in side length will broaden the region where the slot is resonant, thereby increasing the bandwidth of the antenna.

While this idea specifically has not been tried before, there are a few other studies that are similar to what is being proposed. The first one is a trapezoidal slot on the edge of an MSA [4]. The physical construction of this slot is very similar to what is proposed here. However, one key difference is that the study done in [4] uses this slot to broaden the bandwidth of the MSA rather than as its own slot antenna. Another difference is that the way the slot is truncated on the inner edge makes it such that the side lengths of the slot are the same, unlike what is proposed here.

One more study done in a similar area is one with two trapezoidal slots embedded in the center of an MSA [5]. Since the analog to the slanted slot in this thesis is a trapezoidal slot which is discussed and analyzed in Chapter 4, the use of trapezoidal slots in [5] is again physically similar to what is studied here. However, the study in [5] analyzes the behavior of the MSA and not the slots themselves.

To begin, a brief study of half-wave and quarter-wave slots is given in Chapter 2 where several parametric simulations on each antenna are performed in FEKO©. Then Chapter 3 describes the physical construction of the slanted slot and presents the simulations and results of the study. The analogous half-wave version of the slanted slot is a trapezoidal slot contained entirely within a metallic patch. In Chapter 4 this slot is analyzed and compared to the standard rectangular half-wave slot. To conclude this study, Chapter 5 goes through a design example of a slanted slot using the simulations and analyses done in Chapter 3. Several parameters such as operating frequency, bandwidth, and size are specified, and a slanted slot is then designed, simulated, built, and measured. Finally, Chapter 6 summarizes the results of this investigation of slanted slots and outlines several opportunities for future work.

Chapter 2: Background

2.1 Resonant Slot Theory

Prior to the investigation of slanted slot antennas, a basic study of slot antennas was performed. One of the most basic types of antennas is the half-wave dipole antenna, and the complement to that is a half-wave slot antenna. When center-fed, both antennas are resonant at approximately integer multiples of a half-wavelength. The half-wave dipole has a current peak and voltage minimum in the middle, leading to a relatively low impedance at its half-wave resonance. However, the ends of the slot antenna can be thought of as theoretical short circuits. Therefore, there are current maximums at the ends of the slot antenna and a current minimum at the center of the slot. Because of this, there is a very high input impedance at the half-wave resonance if the slot is fed in the middle. However, one way to reduce the impedance of the slot antenna without changing the resonance point is by moving the feed. The current increases closer to the end of the slot, so increasing the feed's offset from the center will lead to a lower impedance. Going back to a center feed, if the frequency of the excitation is increased to where the slot is now a full wavelength long, the center of the slot is a half-wavelength away from a short, and is therefore another short. This causes a current maximum and voltage minimum, which means the feed will see a relatively low impedance at the center.

Another way resonant slot antennas are designed is as a quarter-wave slot. A quarter-wave slot is a slot antenna that uses only one half of the half-wave slot antenna described above. Since a slot "cut" in half inside an infinite metallic sheet is just a smaller rectangular slot, these quarter-wave slot antennas are cut off the edge of a metallic plate. This means there is still a short circuit at the inner end of the slot, but now the end at the edge of the plate acts like an open circuit. This causes a voltage maximum at the open end and a voltage minimum at the short end. Therefore, like with the half-wave slot, moving the feed will cause the input impedance to change, and the larger impedance is close to the open end and the smaller impedance is close to the shorted end. The general relationships between slot size, feed location, and metallic plate size for both antennas are explored in the following sections.
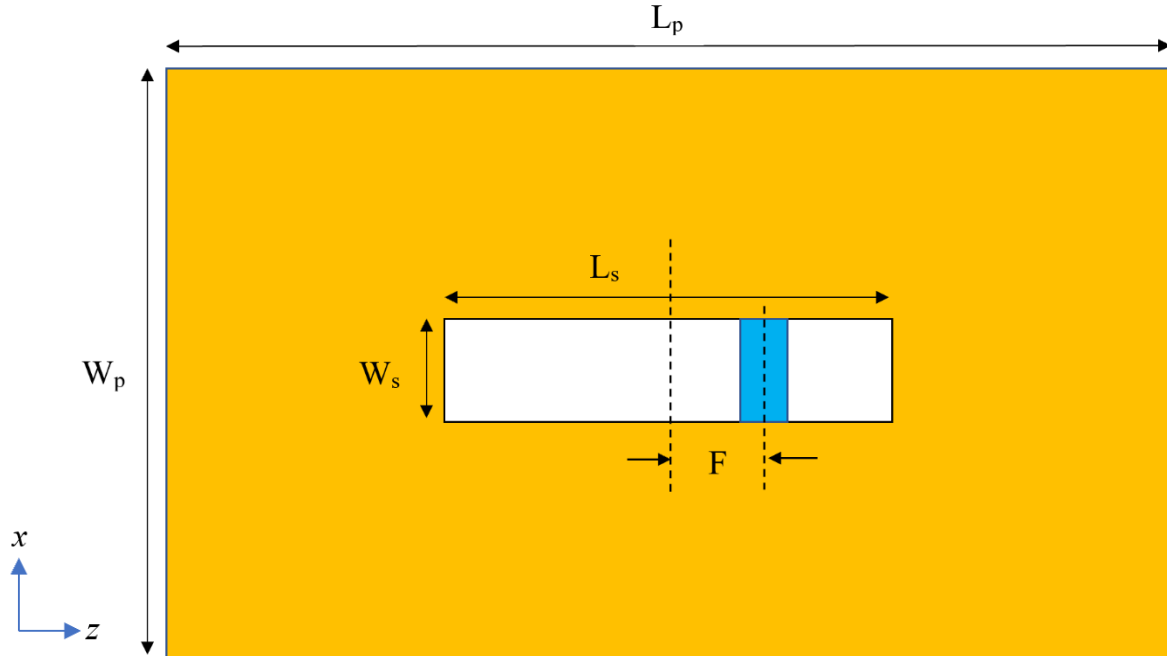
2.2 Half-Wave Slot Antenna Analysis

Figure 2: Physical diagram of the half-wave slot antenna cut out of a metallic plate (gold) and fed (blue) at a distance F away from the center of the slot

The first slot antenna analyzed was the half-wave slot antenna, which is shown with its dimensions labeled in Figure 2. It is a basic rectangular slot cut in a large metallic plate with a simple feed across it, and there were no additional ground planes used. The feed is the blue tab that bridges the slot, which is located a distance F from the center of the slot. In FEKO$^{©}$, this was done by using two narrow metallic tabs to create an edge port which is representative of a semi-rigid coax feed.

First, the radiation pattern for this slot antenna was derived. Using boundary conditions, the tangential electric field at the ends of the slot must be zero, and its distribution across the slot can be given as Equation (1) when the center of the slot is at the origin. In Equation (1) E_0 is some constant electric field, and k is the wavenumber of the excitation, which is equal to $2\pi/\lambda$.

$$E(x,z) = \hat{x}E_0\sin[k\left(\tfrac{L_s}{2} - |z|\right)] \tag{1}$$

The equivalence principle and image theory in Equation (2) was then used to find the magnetic current density distribution along the slot, which is given in Equation (3). In Equation

(2), $\hat{n}$ is the unit vector normal to the surface of the metallic plate. For the $y > 0$ half-space, $\hat{n}$ is equal to $\hat{y}$, and for $y < 0$, $\hat{n}$ is equal to $-\hat{y}$.

$$M = 2E \times \hat{n} \tag{2}$$

$$M(x,z) = sgn(y)\hat{z}2M_0\sin[k\left(\frac{L_s}{2} - |z|\right)] \tag{3}$$

This magnetic current density was then substituted into the equation for the magnetic vector potential, which resulted in Equation (4). After solving that integral and using Equation (5) to find the electric field, the final normalized electric field distribution is given by Equation (6), which matches the result obtained by Kraus and Marhefka in [6] when $W_s \ll \lambda$ and $L_s = \lambda/2$.

$$F = \frac{\varepsilon}{4\pi} \int\int_{\frac{-W_s}{2},\frac{-L_s}{2}}^{\frac{W_s}{2},\frac{L_s}{2}} sgn(y)\hat{z}2M_0\sin[k(\left(\frac{L_s}{2} - |z'|\right)]\frac{e^{-jkR}}{R}dz'dx' \tag{4}$$

$$E = -\frac{1}{\varepsilon}\nabla \times F \tag{5}$$

$$E_\phi = sinc(k\frac{W_s}{2}sin\theta cos\phi)\frac{\cos\left(k\frac{L_s}{2}\cos\theta\right)-\cos(k\frac{L_s}{2})}{sin\theta} \tag{6}$$

After the calculations for the far-field electric field were performed, simulations were run on a half-wave slot to show how the slot's various parameters impact its impedance. All the simulations run on this and following antennas were performed in FEKO©. The default target resonance frequency, a point where the imaginary part of the impedance is zero, for the simulations in this section was 2.4 GHz. The first parametric simulation performed was on the length of the slot. In this simulation $L_p = 175$ mm, $W_p = 150$ mm, $F = 0$, $W_s = 3.13$ mm, and L_s was varied from 45 mm to 63 mm. The resulting impedance from this simulation is shown in Figure 3.

As expected, the resonance frequencies shift downward as the length of the slot is increased. Also, as discussed in the previous section, the real part of the impedance is large at the first resonance but small at the second resonance. The next parametric simulation performed was
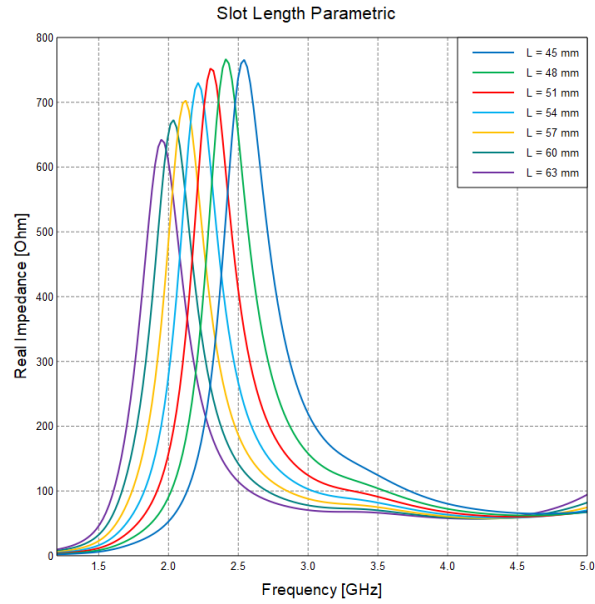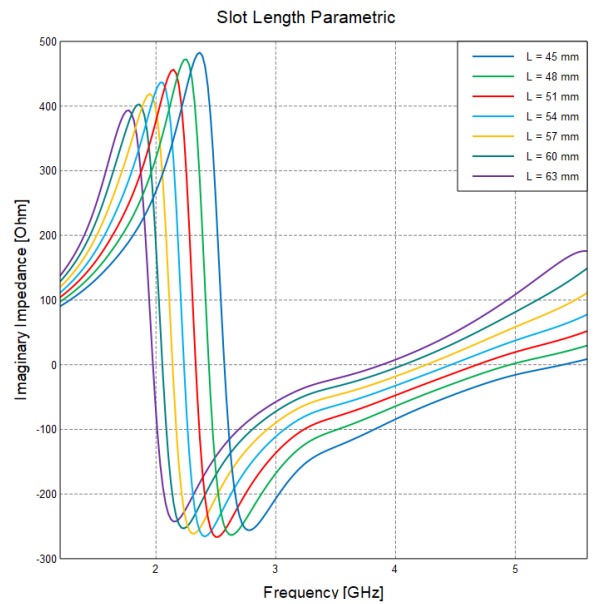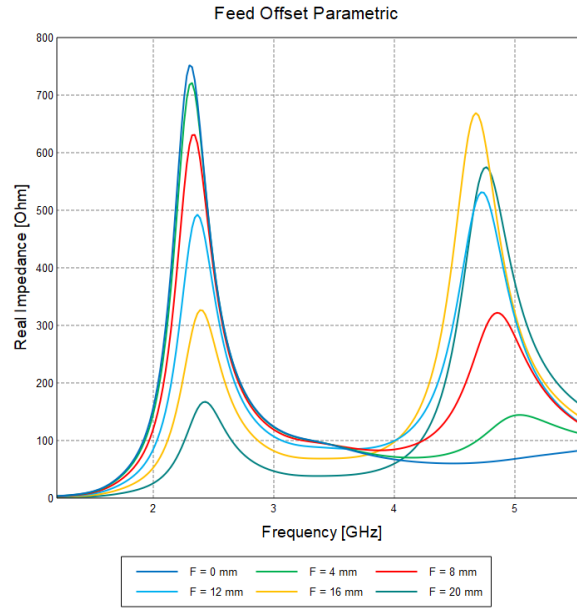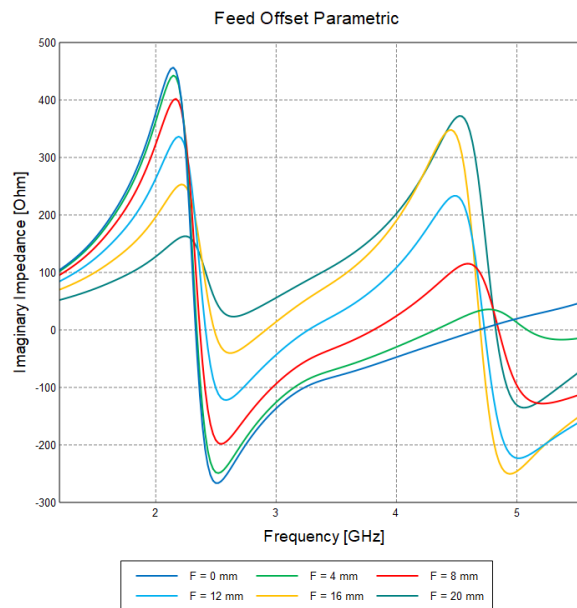
Figure 3: (a) Real part of impedance for the slot length parametric for the half-wave slot. (b) Imaginary part of impedance for the slot length parametric for the half-wave slot.

on the feed location. In this simulation $L_p = 175$ mm, $W_p = 150$ mm, $L_s = 51$ mm, $W_s = 3.13$ mm, and F was varied from 0 to 20 mm.

From Figure 4a we see that as the feed offset increases and the feed shifts towards the edge of the slot, the real part of the impedance decreases at the first resonances and increases at the second resonance. At the first resonance the impedance is large in the center of the slot and small
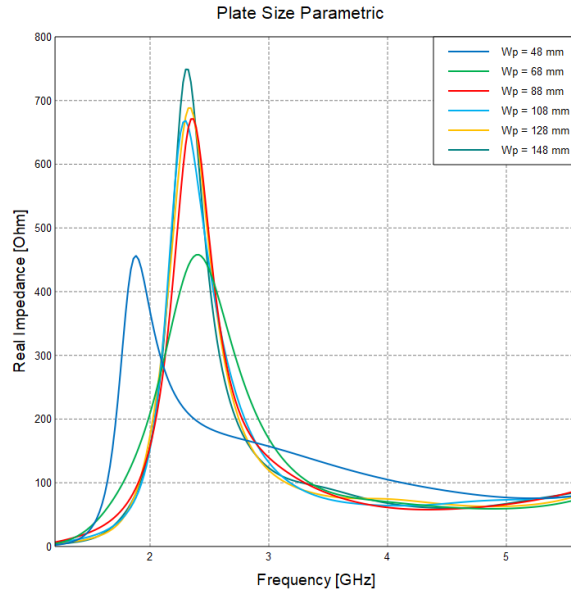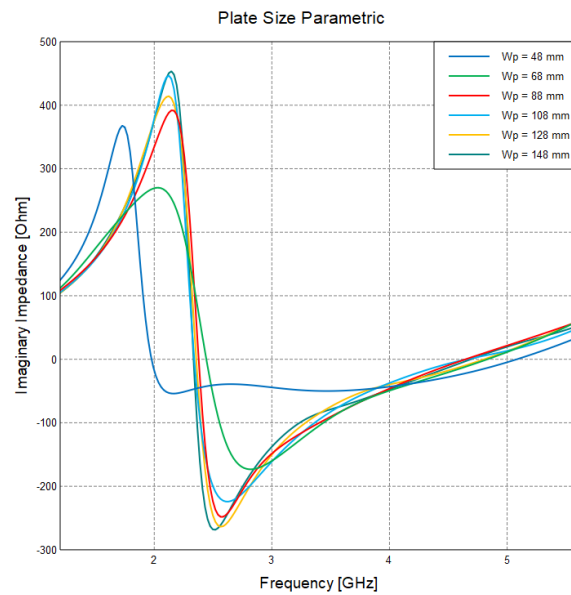
(a)

(b)

Figure 4: (a) Real part of impedance for the feed offset parametric for the half-wave slot. (b) Imaginary part of impedance for the feed offset parametric for the half-wave slot.

at the ends, which explains why it decreases. At the second resonance the impedance starts small in the center of the slot, then increases, peaks, and decreases towards the edge of the slot. Since the edges are essentially short circuits, there are voltage minimums at the ends and in the middle of the slot. As the feed moves from the center towards the end of the slot, it will traverse though a

(a)

(b)

Figure 5: (a) Real part of impedance for plate size parametric for half-wave slot.
(b) Imaginary part of impedance for plate size parametric for half-wave slot.

period of increasing impedance followed by decreasing impedance as it passes over the voltage maximum in between the center and edge.

A similar effect is seen in Figure 4b with the imaginary impedance. However, the overall imaginary impedance also increases as the feed offset increases. This is because as the feed gets closer to the end of the slot, there is more inductance being added from the feed being close to the

theoretical short, which is the end of the slot. Figure 4b also shows that the overall plot for the imaginary impedance for each iteration shifts upwards as the frequency increases. This is due to the inductance seen from the physical feed itself which increases linearly with frequency.

The final parametric study done for the half-wave slot antenna was on the size of the metallic plate. For this simulation, L_p and W_p were scaled together such that L_p was always 1.15 times larger than W_p. The values for this simulation were $L_s = 51$ mm, $W_s = 3.13$ mm, $F = 0$, and W_p was varied from 48 to 148 mm. The resulting impedance plots of the impedance are shown in Figure 5.

From this study it is clear that small plate sizes disrupt the behavior of the slot. For plate sizes only slightly above a half-wavelength, the resonant frequency is shifted away from the desired value. When the plate size is around 0.7λ, the resonance frequency is closer to the target, but the magnitude of the impedance is less than for the rest of the plate sizes. Finally, the slot behaves nearly ideally when the plate size is about 0.8λ or larger.

2.3 Quarter-Wave Slot Antenna Analysis

The next slot antenna analyzed was the quarter-wave slot antenna. The dimensions for this antenna are given in Figure 6. As with the half-wave slot, there is no additional ground plane used for this simulation. The first parametric simulation done was on the feed location. The dimensions of the antenna for this simulation were $L_p = 175$ mm, $W_p = 150$ mm, $L_s = 31.25$ mm, $W_s = 2.5$ mm, and F was varied from 3 to 28 mm. The resulting impedance is shown in Figure 7.

Based on Figure 7a, it is observed that as the feed offset from the open end of the slot increases, the real part of the impedance at the first resonance reduces, which is expected because of the open circuit at the open end of the slot and the short at the other end. In Figure 7a the three-quarter-wave resonance behavior is also observed. At the three-quarter resonance, the voltage distribution will go from a maximum at the open end, pass through a minimum and maximum along the slot and then finish with a minimum at the shorted end of the slot. The impedance at these feed locations for this frequency will therefore first decrease, then increase to the second maximum, and finally decrease again to the inner edge of the slot as F increases. The result of the imaginary part of the impedance shown in Figure 7b shows a result similar to that observed for the half-wave slot in the previous section. As the feed offset increases, the magnitude of the impedance at the first resonance decreases while it increases for the second resonance. Also, the overall
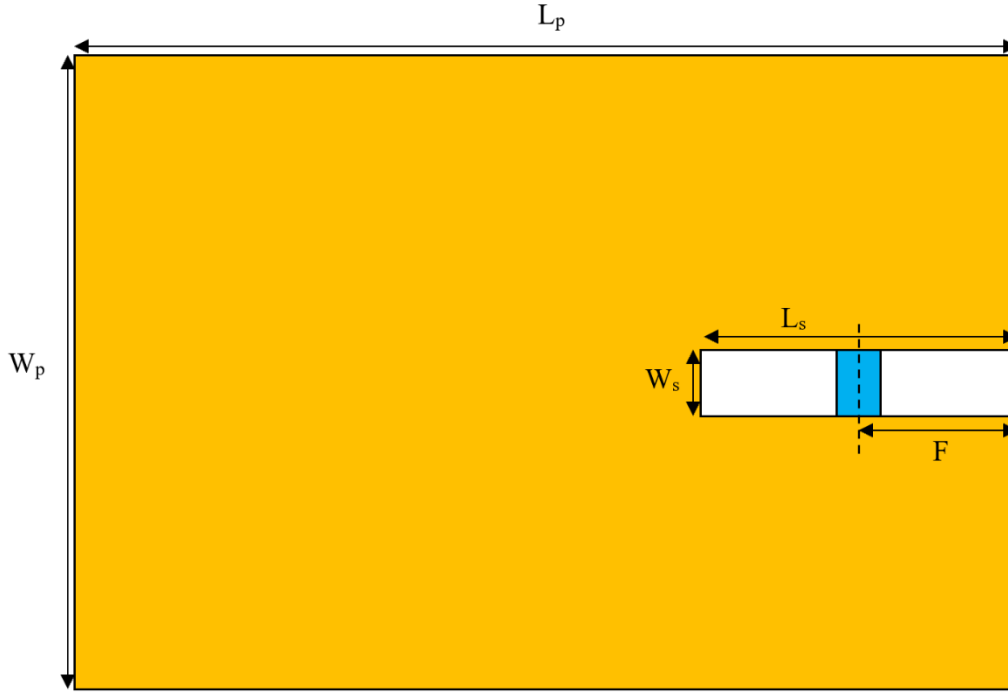
*Figure 6*: Physical diagram of the quarter-wave edge slot

inductance seen increases with the increasing feed offset because the feed is becoming ever closer to the inner end of the slot, which essentially shorts out the input. Lastly, for each feed offset, the inductance increases slightly as the frequency increases due to the inductance in the feed itself.

The second parametric simulation performed was on the length of the slot. The dimensions of the antenna for this simulation were L_p = 187 mm, W_p = 160 mm, W_s = 2.5 mm, L_s was varied from 22.25 to 31.25 mm, and F was changed to keep the F/L_s the same for all iterations so that the resonance location can be observed as a function of slot length only. The resulting impedance simulations for this setup are shown in Figure 8. As expected, the resonance frequency shifts downward as the length of the slot is increased. There is also a large increase in the imaginary impedance as well as leveling-off of the real impedance right at around 2.8 GHz. This phenomenon has been linked to the size of the plate and will be discussed in Chapter 3.

The final study performed on this slot antenna is on the size of the plate. As with the half-wave slot antenna, the length of the plate was kept at 1.15 times larger than the width for each iteration. For this simulation, the dimensions of the antenna were L_s = 31.25 mm, W_s = 2.5 mm, F = 15.13 mm, and W_p was varied from 70 mm to 170 mm.
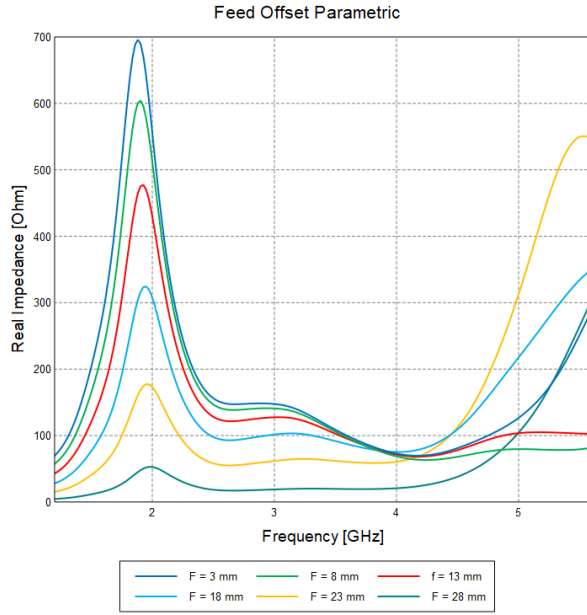
(a)
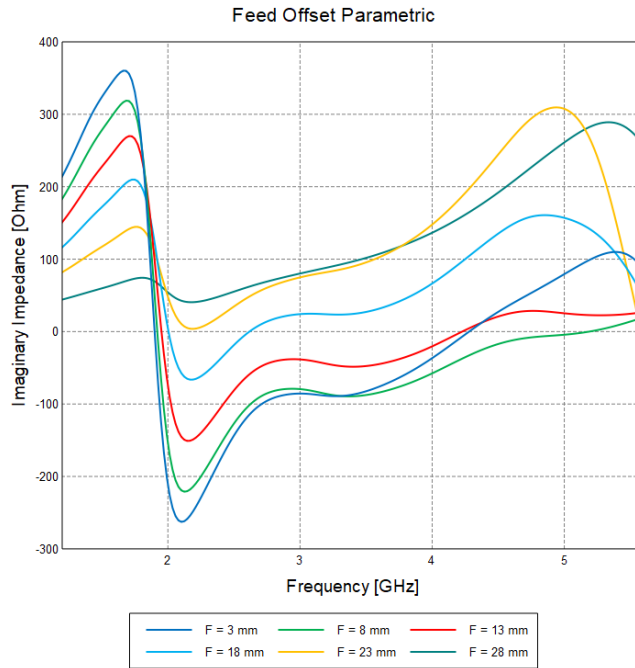
(b)

Figure 7: (a) Real impedance for feed offset parametric for quarter-wave slot.
(b) Imaginary impedance for feed offset parametric for quarter-wave slot.

The resulting impedance plots in Figure 9 show that again for smaller plate sizes, the resonance locations and impedances are significantly disrupted. As the plate size is increased, the slot behaves closer to its typical performance as seen with the first two studies in this section.
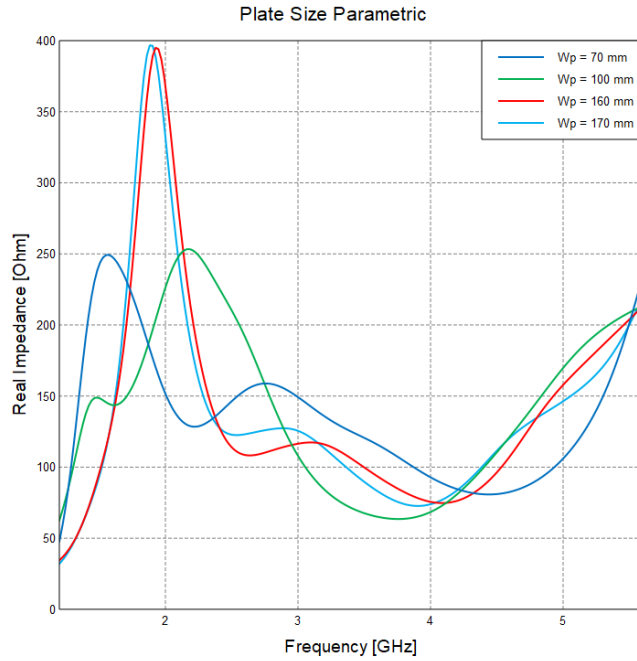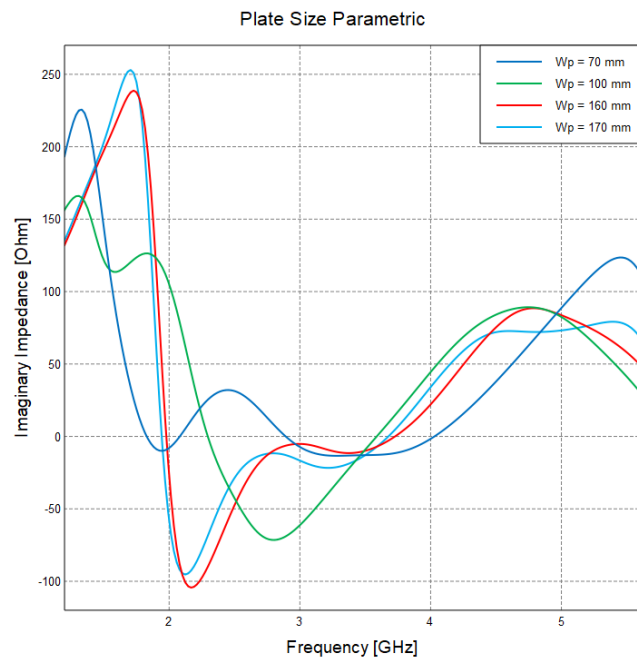
12
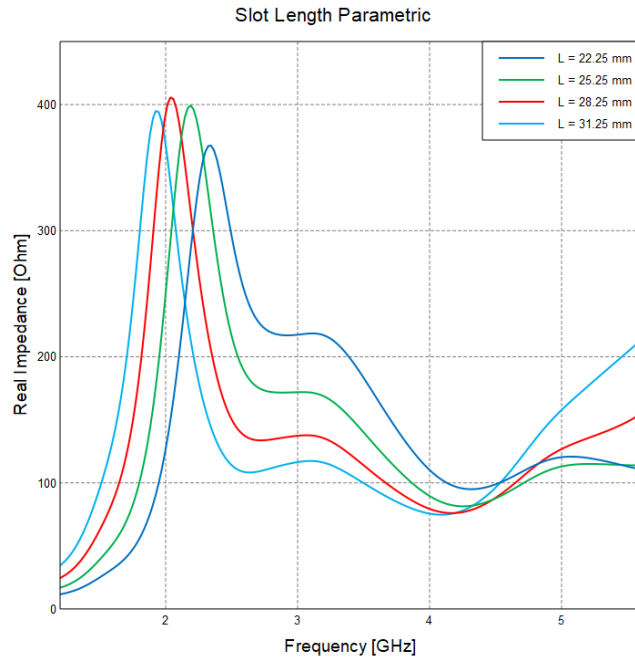
(a)
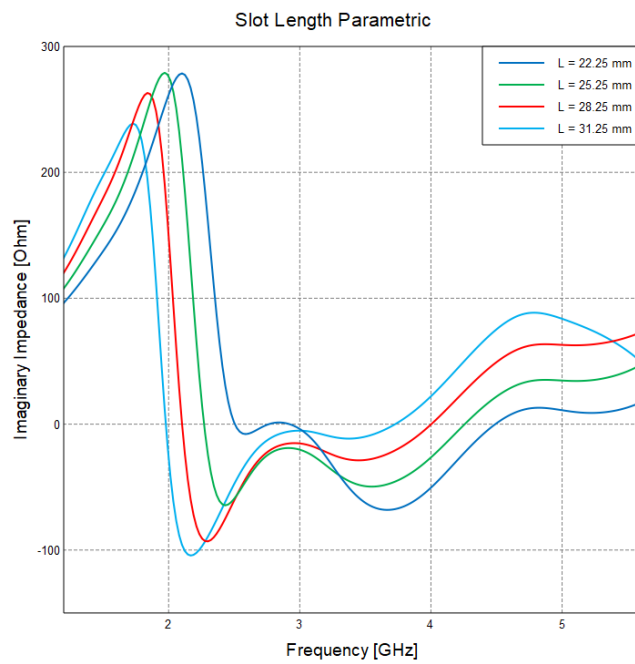
(b)

Figure 8: (a) Real impedance for the slot length parametric for the quarter-wave slot. (b) Imaginary impedance for the slot length parametric for the quarter-wave slot.

(a)

(b)

Figure 9: (a) Real impedance for the plate size parametric for the quarter-wave slot. (b) Imaginary impedance for the plate size parametric for the quarter-wave slot.

Chapter 3: Slanted Edge Slots
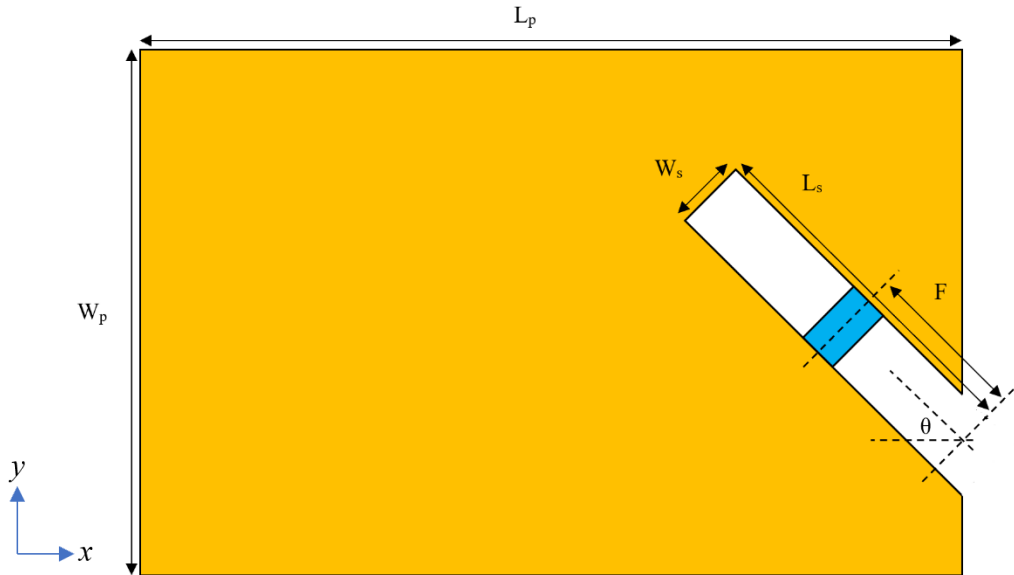
3.1 Physical Diagram

Figure 10: Physical diagram of the slanted slot

This chapter examines the behavior of the proposed slanted slot antenna and compares it to the regular edge slot analyzed in Chapter 2. First, the physical construction of the slot is described, and then the results of several simulations are presented and discussed. The physical layout of the slanted slot with labeled dimensions is shown in Figure 10. As with the previous slots, the blue rectangle is representative of the feed which models a semi-rigid coax feed. There is also no additional ground plane included with this plate for this study. The other dimensions remaining the same from previous studies are the length and width of the plate and the width of the slot.

The main goal of this slanted slot structure is to make the sides of the slot different lengths. As previously discussed, this slot is a resonant structure based on its length, so making this length non-uniform could have interesting implications for the behavior of the slot. In order to make the sides different lengths while keeping the slot width constant, the slot was rotated an angle θ from the horizontal axis as shown in Figure 10. Since the side lengths change with θ, the length of the slot and the feed offset were defined along a line through the middle of the slot which is also

depicted in Figure 10. Therefore, the lengths of the top and bottom side of the slot are given by Equations (7) and (8), respectively.

$$L_{Top,slant} = L_s - \frac{W_s * \tan(\theta)}{2} \tag{7}$$

$$L_{Bot,slant} = L_s + \frac{W_s * \tan(\theta)}{2} \tag{8}$$

From Equations (7) and (8) it is seen that the difference in side length is equal to $W_s * \tan(\theta)$. Therefore, when θ is zero the slot is uniform in length, and the slot is the same as in the rectangular case from Chapter 2. Another implication of the rotation of the slot is that the opening of the slot must also be dependent on θ. Using trigonometry, it is found that the width of the slot opening is given by Equation (9).

$$W_{open} = \frac{W_s}{\cos(\theta)} \tag{9}$$

When θ is zero, the opening is equal to the width of the slot, but as θ approaches 90°, both the width of the opening and the difference in side lengths approach infinity. However, in practice, these values cannot reach infinity because once θ is increased such that the feed has touched the very edge of the plate, the slot cannot rotate any further while still being able to be fed.

3.2 Simulations and Results

The simulations done on the slanted slot were done in a similar fashion to those done on the rectangular half-wave and quarter-wave slots in Chapter 2. Parametric studies were performed on several parameters of the slot to analyze its behavior. Each parametric is then compared to results from the rectangular quarter-wave edge slot and the differences and implications are discussed. The first simulation performed on the slanted slot was a parametric simulation done on θ. The dimensions used for the simulation were $L_p = 176$ mm, $W_p = 160$ mm, $L_s = 30$ mm, $W_s = 2$ mm, $F = 15$ mm, and θ was varied from 0° to 57°. The impedance and S_{11} results for this simulation are shown in Figures 11 and 12, respectively.
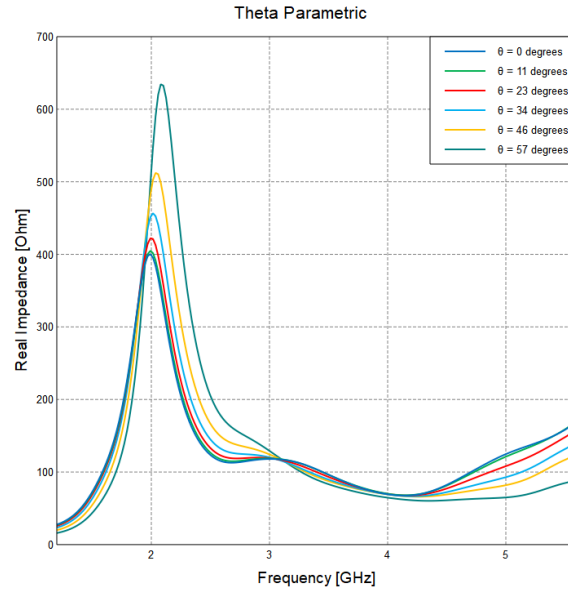
(a)
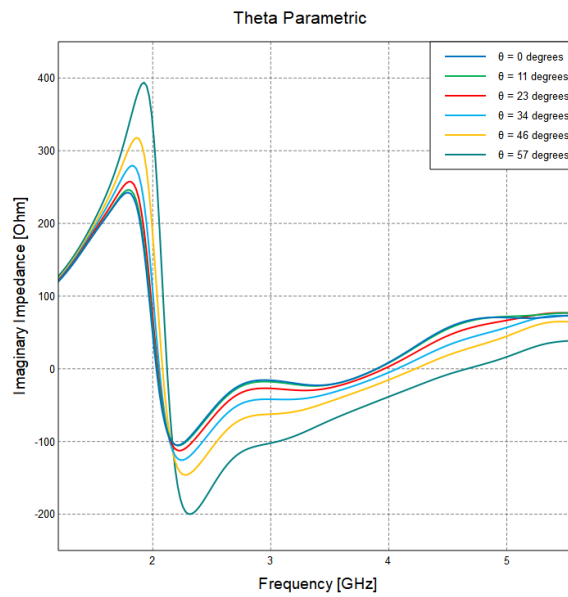
(b)

Figure 11: (a) Real Impedance for the slanted slot θ parametric. (b) Imaginary impedance for the slanted slot θ parametric.

The imaginary impedance in Figure 11b shows that as θ was increased, the resonance frequencies were shifted slightly upward. The first resonance was only slightly increased, but the second resonance experienced a relatively large increase. This shift in resonant frequency can be seen in Figure 11a as well because the peaks of the real part of the impedance shifted slightly upward as θ increased. While these peaks do not determine the resonances, it is known that at the
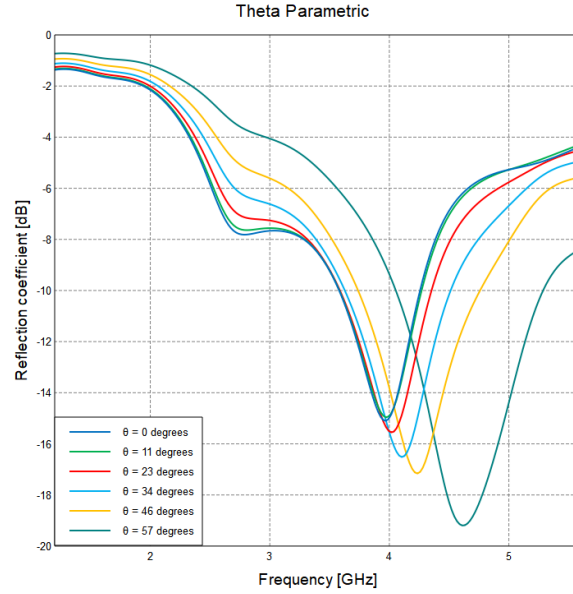
17

Figure 12: S$_{11}$ for the slanted slot θ parametric

first resonance, the voltage and current distributions along the slot lead to a peak in voltage. This means the frequency locations of the peaks are generally correlated with the locations of the resonances.

Since the resonant frequency shifted upwards, it indicates the effective length of the slot decreased as θ was increased. It was found that the value of the wavelength for the first resonance frequency was about four times larger than the shorter side length of the slanted slot. This shows that the behavior of the resonance locations for the slanted quarter-wave slot are determined by the length of its shorter side.

It was also hypothesized that a slanted slot would have a larger bandwidth because its length is no longer uniform. The bandwidth is measured to be the frequency range over which S$_{11}$ is less than or equal to -10 dB with a reference impedance of 50 Ω, which approximately equates to when the normalized impedance on the Smith chart is within the VSWR = 2 circle. This region will be called the "matched region" throughout the rest of this thesis. It is observed in Figure 12 that the bandwidth appears to increase as θ increases. It is also seen that that the center frequency of the bandwidth also shifts upward as θ increases and is approximately equal to the frequency of the second resonance of the slot. The values of the center frequency, bandwidth, and fractional bandwidth (FBW) are given in Table 1. Fractional bandwidth is calculated as the bandwidth divided by the center frequency.

Table 1: Center frequency and bandwidth for slanted slot θ parametric

Theta (degrees)	Center Frequency (GHz)	Bandwidth (MHz)	FBW (%)
0	3.97	676.9	17.1
11	3.98	688	17.3
23	4.03	766.6	19
34	4.1	885.6	21.6
46	4.25	1,020.80	24
57	4.62	1,232.30	26.7

Table 1 shows that as θ increases, the bandwidth and the fractional bandwidth also increase. This simulation confirms the idea that putting the slot on a slant will increase the bandwidth of the antenna. An important note here is that while both the bandwidth and FBW are increasing, the more important result is that the FBW is increasing because this metric takes into consideration the center frequency of the matched region. Since the resonant frequencies increase when the slot is put on a slant, one would have to make the slanted slot slightly longer than the rectangular slot to achieve the same center frequency.

When the slot is put on a slant, the side lengths become different, but the physical location and orientation of the slot within the plate change as well. It was observed that changing θ produced a significant impact on the impedance and location of the resonances for the slanted slot. Therefore, in order to isolate the effects of the side lengths from the interaction with the plate, the "knife edge" slot design in Figure 13 was simulated. This knife edge slot is the same as the rectangular slot, except one side of the slot is extended by $W_s*\tan(\theta)$, which is the same as the side length difference determined by Equations (7) and (8).

The simulated S_{11} of the knife edge slot with θ equal to 45° is shown in Figure 14. From this plot, it was determined that the center frequency and the bandwidth are 3.97 GHz and 727.4 MHz. This center frequency exactly matches the center frequency of the regular edge slot from Table 1, however the bandwidth is noticeably larger. This indicates that the difference in long side length is directly responsible for the increase in bandwidth of the slot which is precisely what was predicted. Another important note for this design is that the length of the short end was kept the same as the length of the rectangular slot, which further confirms that the resonance of a slot with different side lengths is more strongly dependent on the length of the shorter side.
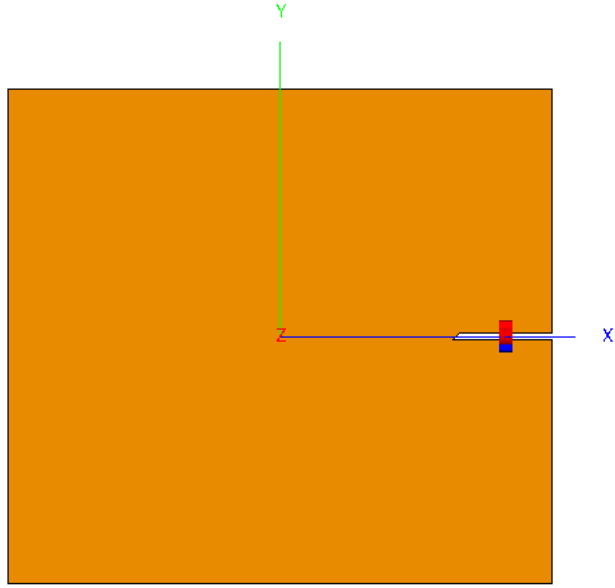
19

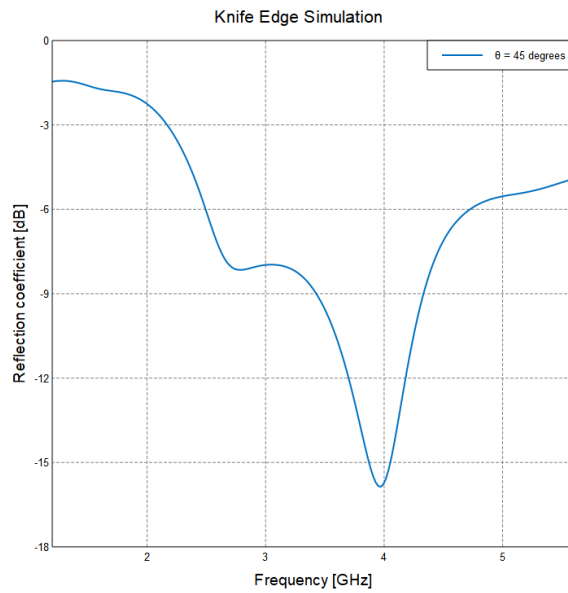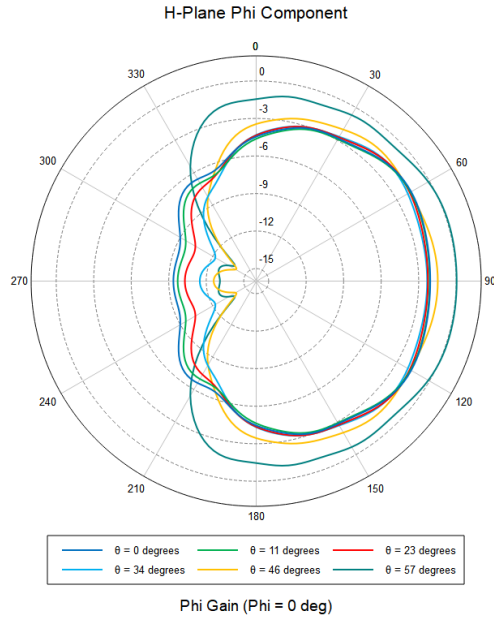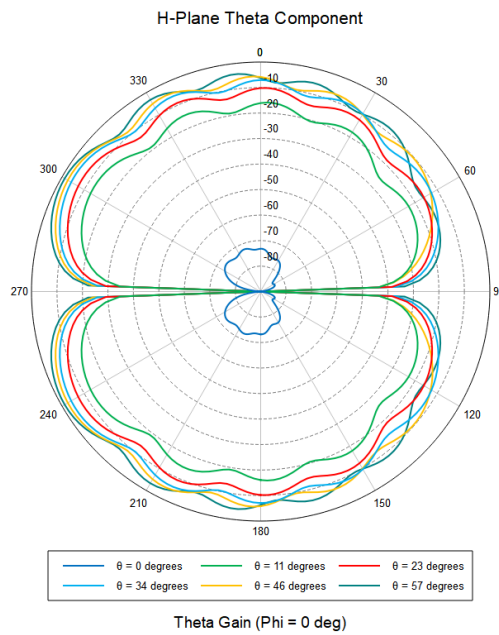*Figure 13*: Physical diagram of knife edge slot

Figure 14: S_{11} for knife edge simulation

While the bandwidth and center frequency are two important characteristics of an antenna, another important performance metric is its radiation pattern. The far-field radiation patterns for the E-plane and H-plane for slots at the various angles in this study are given in Figure 15. The radiation patterns are all given at the center frequency of the matched region. Since we now have a θ defined for the angle of the slot, and another Theta describing the angle in spherical coordinates, the symbol θ will refer to the angle of the slot and the word Theta will refer to the coordinate angle.

H-Plane Phi Component

Phi Gain (Phi = 0 deg)

(a)

H-Plane Theta Component

Theta Gain (Phi = 0 deg)

(b)

Figure 15: Far-field radiation for various θ (a) The H-plane Phi component. (b) The H-plane Theta component. Continued on 22.

When examining the H-plane (Phi = 0°) radiation in Figure 15a, the pattern is symmetric for all values of θ. The gain of the antenna is relatively constant when θ is small, but once θ becomes larger than about 45°, the gain increases and becomes more uniform. For the E-plane (Phi = 90°) in Figure 15b, however, only the rectangular edge slot is symmetric. As θ increases, the

E-Plane Phi Component

Phi Gain (Phi = 90 deg)

(c)

E-Plane Theta Component
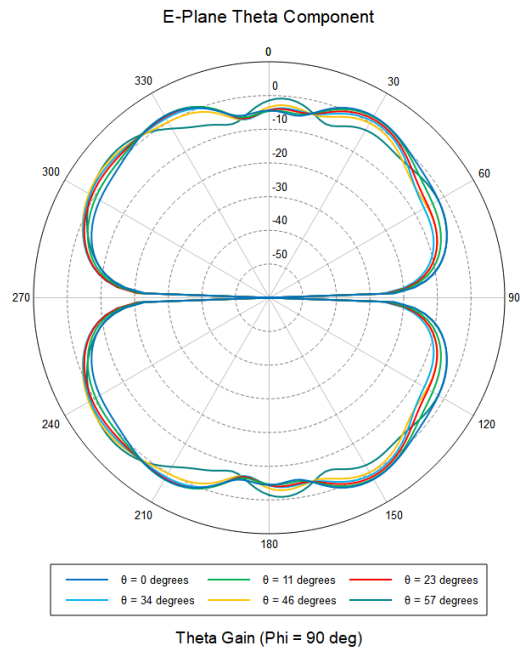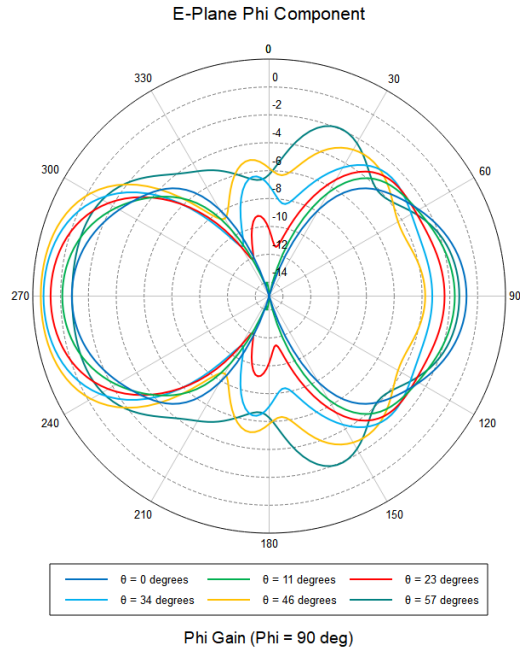
Theta Gain (Phi = 90 deg)

(d)

Figure 15 continued. (c) The E-plane Phi component. (d) The E-plane Theta component.

beam becomes steered towards the direction the slot is pointing. This means that while the gain of the antenna experiences minor changes, the biggest impact of the slot on the radiation pattern is for the main direction of the beam.
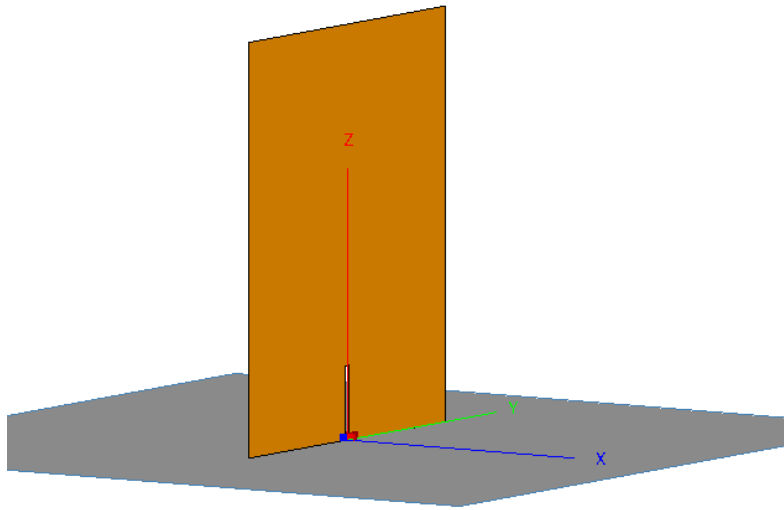
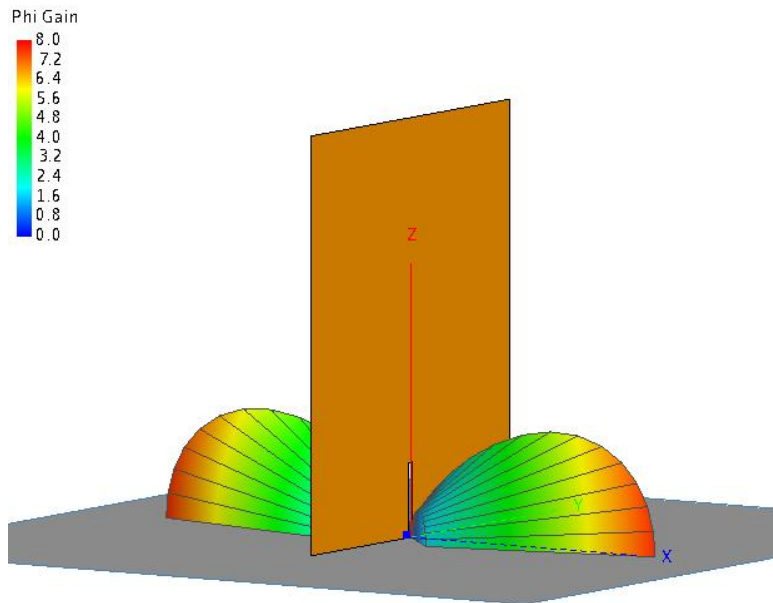*Figure 16*: Physical diagram of a rectangular edge slot above a PMC

Figure 17: Radiation pattern for a rectangular edge slot above a PMC

However, the radiation pattern of these edge slots looks much different than one would expect of a typical slot antenna. The beam is angled more towards the open end of the slot rather than broadside. This is because while the quarter-wave slot is acting as the dual to a monopole, it is missing one key piece that monopoles have, which is a ground plane. Because this slot antenna has nothing to produce the requisite images that cause the manifestation of the proper radiation pattern, the actual radiation pattern is angled towards the opening of the slot and has no null in the XY-plane on the side with the slot opening. In order to further test this idea, a simulation of this
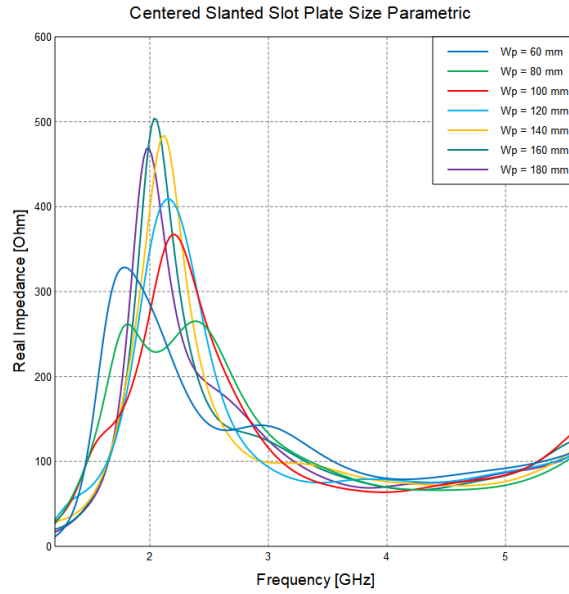
(a)
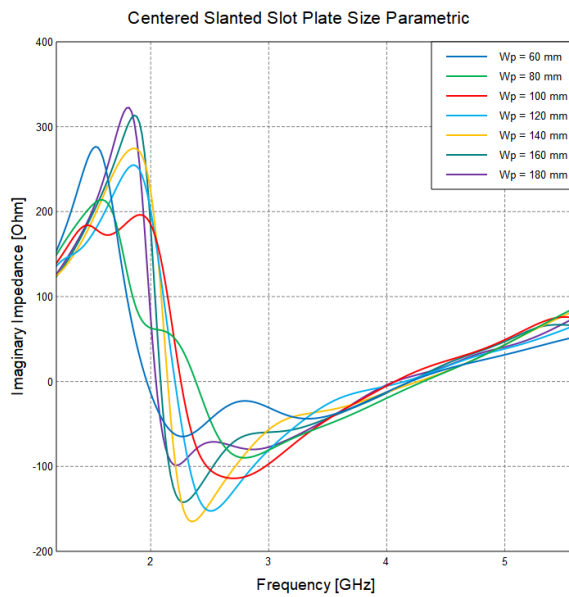
(b)

Figure 18: (a) Real impedance for the centered slanted slot plate size parametric.
(b) Imaginary impedance for the centered slanted slot plate size parametric.

slot with an infinite PMC placed perpendicular to the opening of the slot was performed. The setup and radiation pattern are shown in Figures 16 and 17, respectively.

The reason a PMC is used instead of a PEC is that this slot monopole is the dual of a metallic monopole. While a PEC creates the proper images for the currents in a monopole to produce the correct radiation pattern, a PMC is needed to likewise create the proper images for the
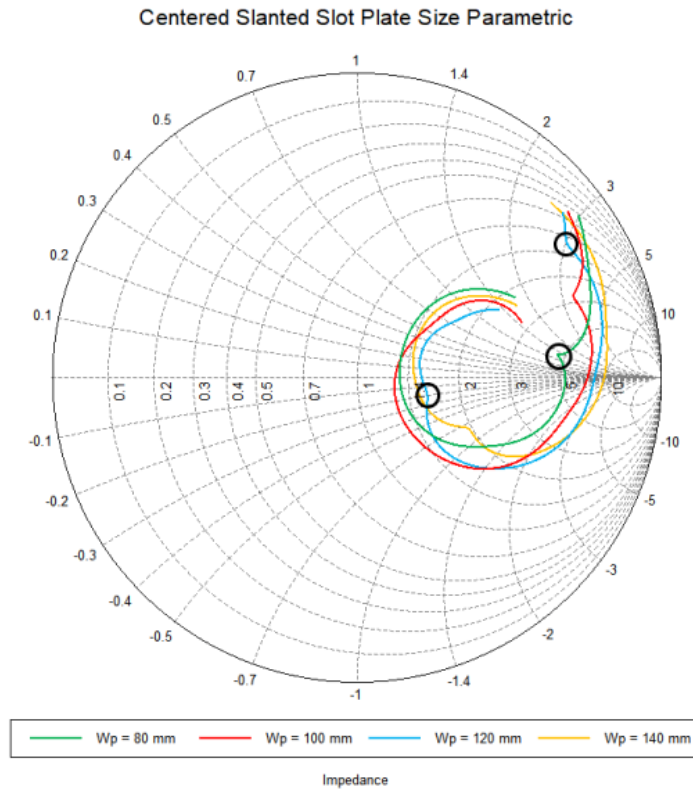
Figure 19: Smith chart showing notches for the centered slanted slot plate size parametric over a frequency range of 1.2 GHz to 5.6 GHz

magnetic currents within the slot. This is confirmed by the expected radiation pattern of a half-wave dipole being produced in Figure 17.

While the change in side lengths resulted in an increased bandwidth, there is clearly still an impact from the change in the slot location and orientation within the plate. In order to investigate what this impact might be, a parametric simulation was run on the plate size of the slanted slot. The dimensions of the slot for this simulation were $L_s = 30$ mm, $W_s = 2$ mm, $\theta = 45°$, $F = 15$ mm, W_p was varied from 60 mm to 180 mm, and L_p was adjusted such that L_p/W_p was kept at a constant ratio of 1.1. The resulting antenna input impedance of this simulation is given in Figure 18.

From Figures 18a and 18b, it is clear the plate size has a sizeable impact on the performance of the slot as expected from the preliminary study in Chapter 2. For smaller plate sizes where W_p is less than 100 mm, the resonance locations are significantly affected and vary widely while the real part of the impedance also exhibits shifts in the location of the peak or even has multiple peaks. For plate sizes where W_p is greater than 100 mm, the resonances still shift slightly, but they are

Table 2: Location of notches for various plate sizes

| Plate Size (mm)	Lower Notch		Upper Notch	
	Frequency (GHz)	Electrical Plate Size at Notch Frequency (λ)	Frequency (GHz)	Electrical Plate Size at Notch Frequency (λ)
60	2.78	0.556	-	-
80	2.06	0.549	-	-
100	1.64	0.547	-	-
120	1.37	0.548	3.86	1.544
140	-	-	3.31	1.544
160	-	-	2.87	1.531
180	-	-	2.52	1.512

smaller and more predictable changes. This shows that, as expected, the larger the plate size the better the performance of the slot.

When running the plate-size parametric simulation, another phenomenon was observed. In the plot of the normalized impedance on the Smith chart for this simulation in Figure 19, various "notches" were discovered. These notches were found to rotate around the Smith chart clockwise as the size of the plate increased. This corresponded to the location of a notch shifting downwards in frequency as the plate size was increased. It was also discovered that for certain plate sizes, a second notch at a separate frequency could be seen in one trace. Once the locations of the notches in frequency were mapped out according to the plate size, it was found that they occurred at frequencies where the plate width, W_p, was an odd-integer multiple of a half-wavelength. Table 2 lists the location of these notches and the electrical length of the plate width at the frequency where the notch is located.

This discovery indicates that the notches seen are a result of the resonance of the plate in the direction along the width of the plate, however, only at resonances where there is a maximum current at the center. According to the dipole theory discussed in Chapter 2, the ends of the metallic plate appear as open circuits, so when an excitation is at the frequency where the plate is a half-wavelength long, there will be a voltage minimum and current maximum at the center. When the excitation becomes such that the plate is a full wavelength, then the voltage will cycle from a maximum to minimum, to maximum at the center, to minimum, and back to another maximum at the open circuit at the other end of the plate. Since the feed across the slot is in the middle of the plate, the voltage and current distribution produced by the plate in the middle of the plate will also
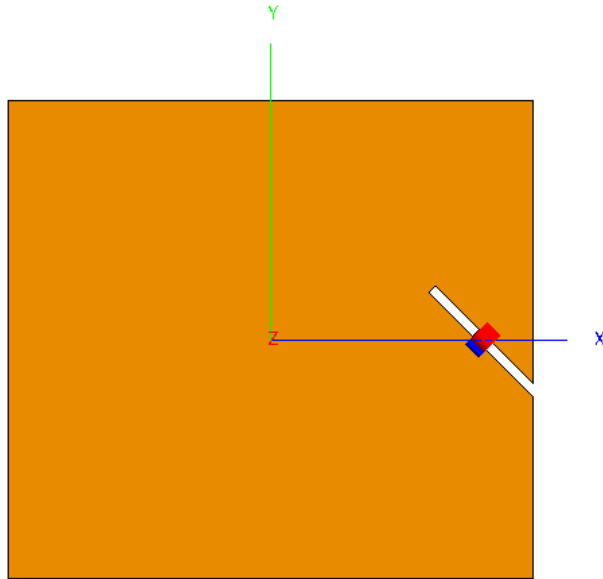
(a)
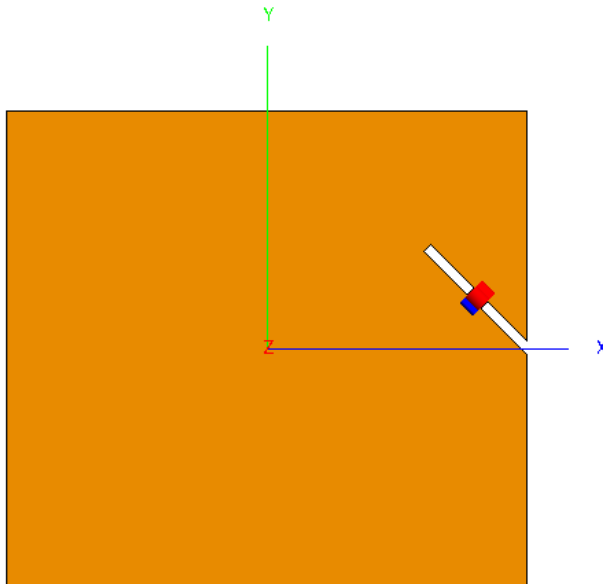
(b)

Figure 20: (a) Physical layout for the centered slanted slot. (b) Physical layout for the centered opening slanted slot. The red and blue segments within these slots represent the positive and negative ends of the feed, respectively.

have a contribution. For an infinite plate, there would be no resonance from the plate, and only the distribution from the slot would impact the results. However, for a finite plate, the specific plate size plays a role.

When the wavelength of the excitation is such that the plate is an even-integer of a half-wavelength, there will be a voltage maximum and current minimum created by the plate at the center. Since this corresponds to a large impedance, it is essentially a large impedance from the

plate in parallel with the impedance from the slot. This approximately equals the impedance of the slot, so minor to no distortions from the plate are seen around these frequencies. However, when the wavelength of the excitation is an odd-integer multiple of a half-wavelength, there is a voltage minimum and current maximum at the center. This corresponds to a low impedance, which will combine in parallel with the impedance of the slot. In this case, the low impedance from the plate reduces the overall impedance of the antenna which manifests itself in the form of the notch.

Because the plate size and location of the slot and feed along the width of the plate matter, the same plate size parametric study was performed on a slot with a centered opening as well as for the regular rectangular edge slot. Figure 20a shows how the slot for the original parametric was placed so that the physical slot was centered along the width of the plate. For the next simulation, the opening of the slot was centered as shown in Figure 20b. The rest of the slot dimensions were kept exactly the same for each iteration of the plate size. The normalized impedances on Smith charts from these two parametric simulations, as well as a plate size parametric simulation on a regular rectangular edge slot, are shown in Figures 21-23.

As seen in these plots, the centered slot and centered opening slanted slot plate size parametric simulations produce very similar results. However, both slanted slot simulations are much different than the rectangular edge plate size parametric. The traces for the various plate sizes in the Smith chart in Figures 21 and 22 are all more bunched together than those in Figure 23. This indicates that having the slot on a slant helps reduce the impact of the plate size on the behavior of the slot because the impedances are more consistent for the slanted slots.

It is also observed in the S_{11} plots in Figures 24-26 that the center frequencies and bandwidths remain more consistent for the slanted slots than for the edge slot. In general, the bandwidths are all centered around approximately the same frequency, which shows that the plate is ultimately not responsible for determining the location of the matched region. However, the plate size does affect the bandwidth of the slot. Table 3 lists the center frequency and FBW for each of the slanted slot simulations and the rectangular edge slot simulation. There is not much difference between the centered slanted slot and the centered opening slanted slot, so this discussion focuses on the slanted slots as a group compared to the edge slot, rather than the three of them separately.

From this table, it is observed that the location of the matched region is shifted upwards when the slot is put on a slant. This increase in resonance frequency for larger θ was also
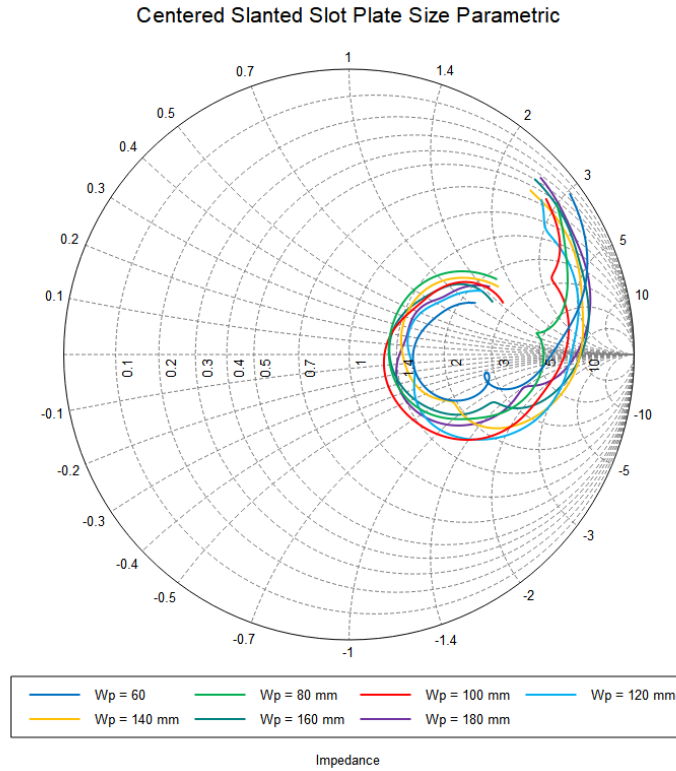
28

Figure 21: Smith chart results for the centered slanted slot plate size parametric over a frequency range of 1.2 GHz to 5.6 GHz
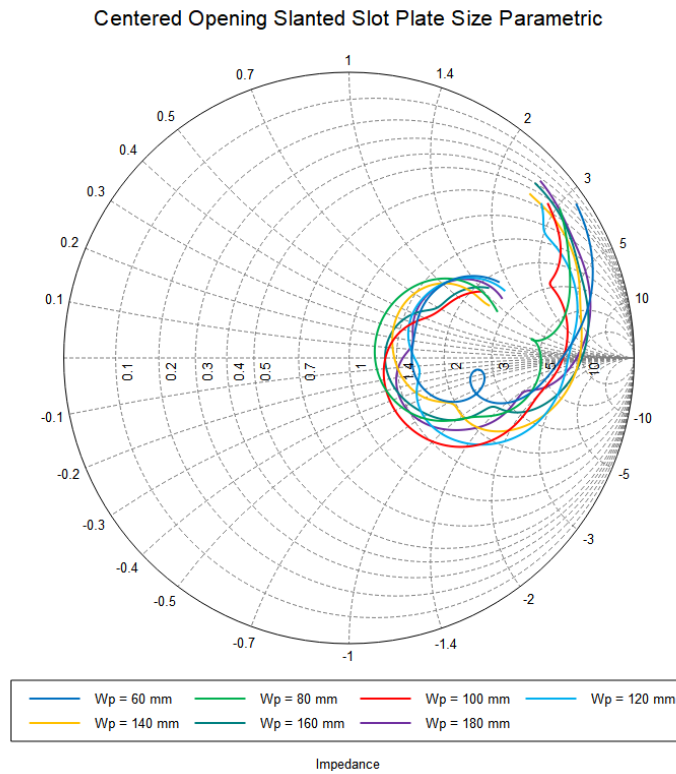

Figure 22: Smith chart results for the centered opening slanted slot plate size parametric over a frequency range of 1.2 GHz to 5.6 GHz
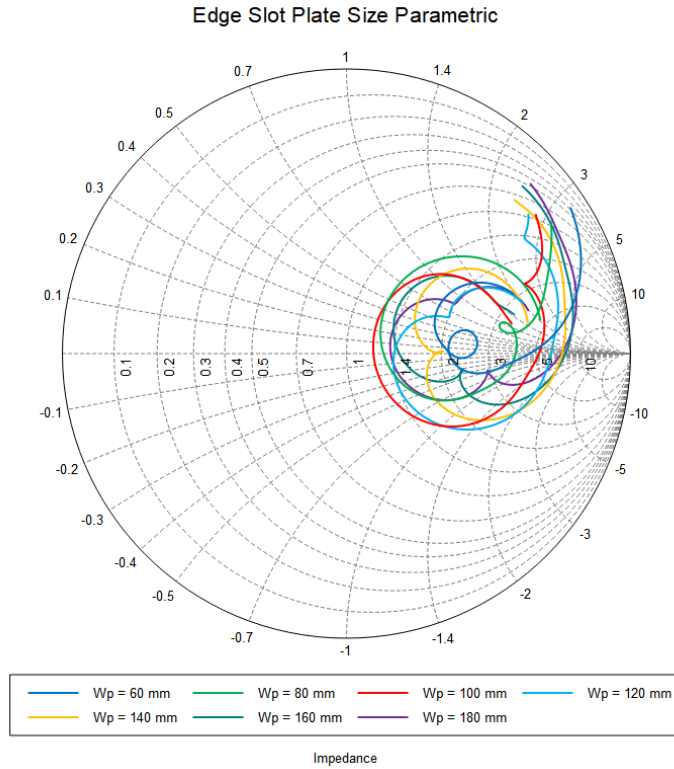
Figure 23: Smith chart results for the regular edge slot plate size parametric over a frequency range of 1.2 GHz to 5.6 GHz
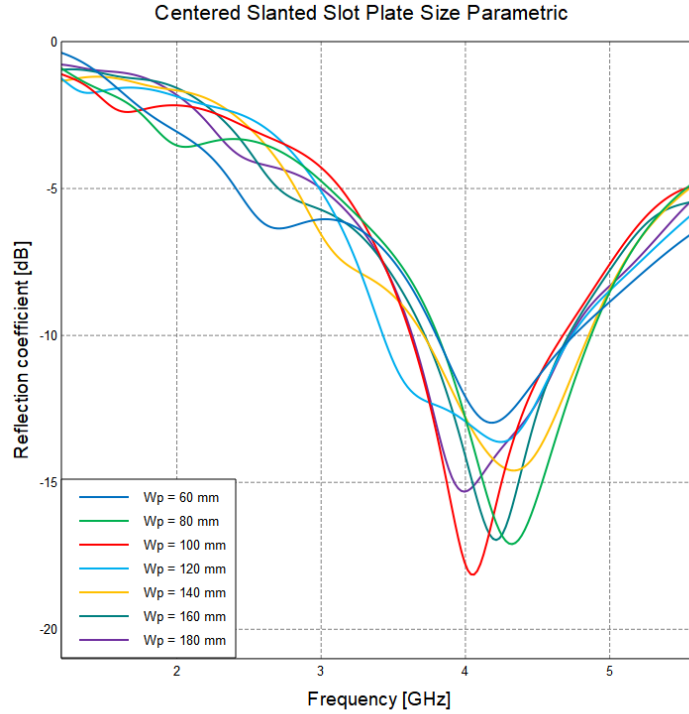

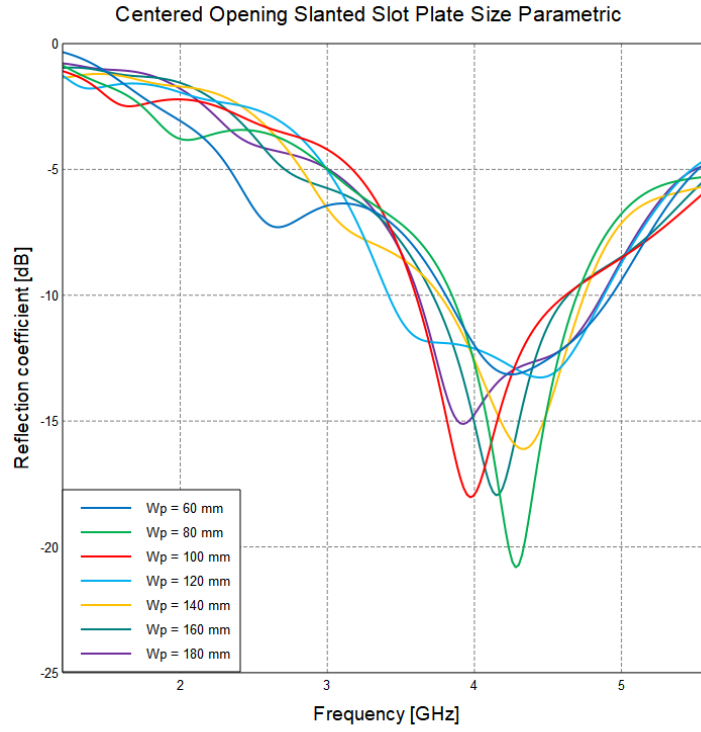*Figure 24*: S$_{11}$ for the centered slanted slot plate size parametric

30

Figure 25: S$_{11}$ for the centered opening slanted slot plate size parametric
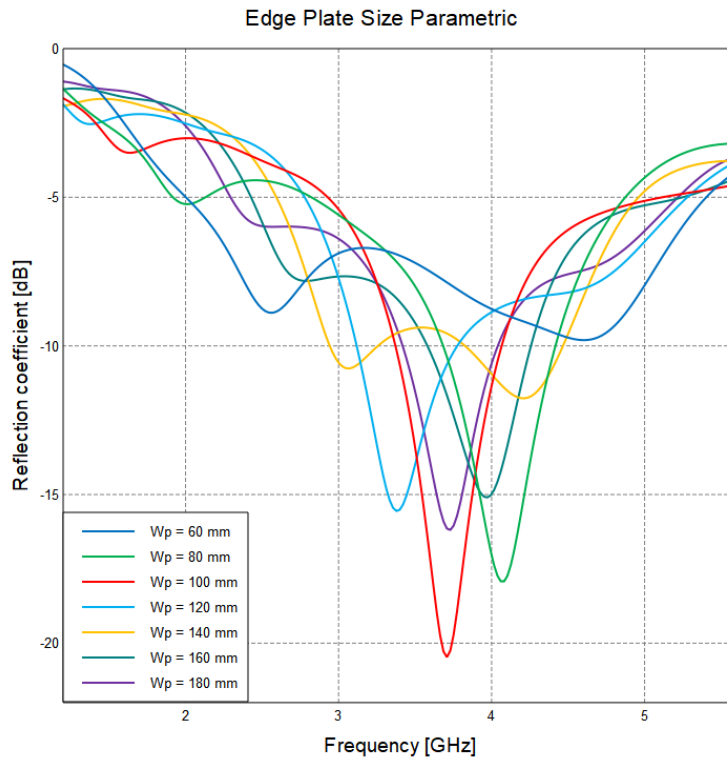

Figure 26: S$_{11}$ for the rectangular edge slot plate size parametric

31

Table 3: Comparison of center frequency and FBW for the three plate size parametrics

Plate Size (mm)	Edge		Centered Slot		Centered Opening	
	Center Frequency (GHz)	Fractional Bandwidth (%)	Center Frequency (GHz)	Fractional Bandwidth (%)	Center Frequency (GHz)	Fractional Bandwidth (%)
60	-	-	4.19	22.7	4.26	26.5
80	4.08	18.0	4.32	24.6	4.29	19.8
100	3.71	18.7	4.06	26.0	3.98	25.6
120	3.39	19.4	4.09	32.0	4.15	35.3
140	3.71*	41.0	4.34	26.3	4.34	22.6
160	3.97	17.1	4.21	23.7	4.16	22.1
180	3.73	16.7	4.19	26.2	4.25	29.5

discovered in the parametric study previously done on θ, which helps to further prove its legitimacy. The center frequencies for the regular edge slot range from 3.39 GHz to 4.09 GHz while the center frequencies for the slanted slots are between 3.98 and 4.34 GHz. So not only does the entire range shift upwards, but there is less variation in the center frequency for the slanted slots. This result gives numerical proof to the observation from the Smith charts in Figures 21-23 that the slanted slots produce more consistent behavior for varying plate sizes.

Tables 2 and 3 together show the link between the notch and its potential impact on the bandwidth. Since the notch is the result of the resonance of the plate at a low impedance combining in parallel with the impedance seen by the slot, the notch tends to cause a small dip in the reflection coefficient where it occurs. This dip is normally small, so the curve deviates little from the slot's normal behavior. However, when the notch is located close to the matched region, the dip it creates in S_{11} extends the bandwidth. When the plate size has a width of 120 mm, the FBW of the slanted slots see a sudden jump. This is because the notch is located on the lower end of the matched region, and as seen with the light blue trace in Figures 24 and 25, the matched region is extended because of this.

For the regular edge plate, this phenomenon occurs when the plate width is 140 mm because the center frequencies are lower for this slot and larger plate sizes mean lower notch frequencies. As seen with the yellow trace in Figure 26, the bandwidth again is extended. There is an asterisk next to this center frequency because this matched region is not technically continuous. It briefly rises above the -10 dB threshold, before dropping below again. For this table, however, it was treated as one full band to better analyze the data. While the FBW for this case is significantly larger than the others, it would technically be lower if the plate or slot size was slightly adjusted so that the resonance overlapped better. Even with this reduction, an important note is

that the sudden increase in bandwidth from the notch will have a larger impact on the rectangular edge slot than on the slanted slots. This can be seen to be true in Figures 21-26 because the notches in the Smith charts and dips in the S_{11} plots are much more pronounced for the rectangular edge slot than for the slanted slots. The implication of this result is that if one would like to design a rectangular slot with as much bandwidth as possible and one has control over the size of the plate and the slot, designing the plate resonance to be near the slot resonance will significantly extend the bandwidth.

In conclusion, this study of slanted slots shows that as the slant angle increases, the bandwidth and resonant frequencies increase slightly while the radiation pattern also shifts off-center. It also showed that the behavior of a slanted slot will be more robust to changes in the size of the metallic plate it is located in. The plate-size parametric also showed that the resonance of the plate will have an impact on the slot, and when it is located near the second resonance, it can enhance the bandwidth. This means that an antenna designer can achieve much larger bandwidth by placing the slot on a slant as well as carefully selecting the size of the plate. But it also shows that if the designer does not have control over the size of the plate, a slanted slot can be used to get more bandwidth while also being more consistent than a rectangular slot.

Chapter 4: Trapezoidal Slots
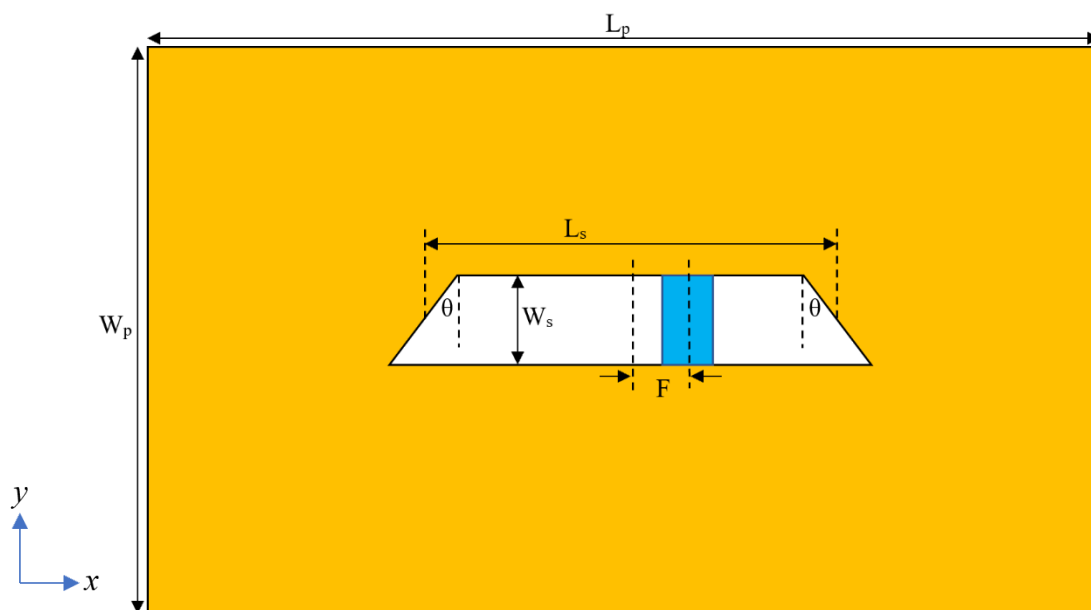
4.1 Physical Diagrams

Figure 27: Physical diagram for the trapezoidal

In Chapter 2 it was discussed that a quarter-wave monopole can be translated to a half-wave dipole, and likewise a quarter-wave slot monopole can be translated to a half-wave slot. When the slanted slot is translated to its half-wave counterpart, it creates a trapezoidal slot. Alongside the study of the slanted slot, a study of the analogous trapezoidal slot was performed. The physical diagram of the trapezoidal slot is shown in Figure 27.

Consistent with the other studies, there was no additional ground plane added, and the blue rectangle represents the semi-rigid feed used to feed the structure. Also as before, L_p and W_p are the length and width of the plate, respectively. W_s is the width of the slot, and F is the location of the feed relative to the center of the slot. L_s is the length of the slot but, as with the slanted slot, is defined to be the length along the middle of the slot. In order for this slot to be the equivalent analog, θ is defined to be the upper angle in the triangles that form the ends of the trapezoid.

It can be shown that this slot is the half-wave version of the slanted slot for the same values as θ so long as $L_{s,trap} = 2L_{s,slant}$ and W_s is the same for both slots. The simplest case is that when θ

is zero, the length of the trapezoidal slot will be uniform and equal to $L_{s,trap}$, and the length of the rectangular slot will also be uniform and equal to $L_{s,slant}$ which is half the trapezoid. Using trigonometry, it can be found that the lengths of the top and bottom of the trapezoid are equal to those given in Equations (10) and (11).

$$L_{top,trap} = L_{s,trap} - W_s * \tan(\theta) \tag{10}$$

$$L_{bot,trap} = L_{s,trap} + W_s * \tan(\theta) \tag{11}$$

For the conditions listed in the preceding paragraph, Equation (7) is exactly half of Equation (10) and Equation (8) is half of (11). Also using Equations (10) and (11) it is easily seen that the difference in side length for this slot is $2*W_s*\tan(\theta)$ which is twice the side length difference found for the slanted slot in Equation (9). Since the top, middle, and bottom of the trapezoidal slot have been shown to be twice the length of the top, middle, and bottom of the slanted slot, we can be sure this is the correct half-wave analogue to the slanted slot.

4.2 Simulations and Results

A study similar to that performed on the slanted slot in Chapter 3 was done on this trapezoidal slot. First, a parametric simulation was done for θ, and then another was done on the plate size of the antenna. These results were then compared with a regular rectangular half-wave slot, and also with the results attained from the slanted slot study. For the parametric study on θ, the dimensions of the plate were $L_p = 175$ mm, $W_p = 150$ mm, $L_s = 51$ mm, $W_s = 2.5$ mm, $F = 8$ mm, and θ was varied from $0°$ to $72°$. The resulting impedance plots from this simulation are shown in Figure 28.

From these plots we can see that when θ first increases, the resonant frequencies slightly decrease, but then as θ gets larger, the frequencies decrease at larger rates. This is expected because for linear steps in θ, the side lengths change by non-linear steps caused by the mapping of $\tan(\theta)$. Since the feed is offset for this parametric, there are two peaks in the real part of the impedance, one at approximately the half-wave resonance and the other at the full-wave resonance. This
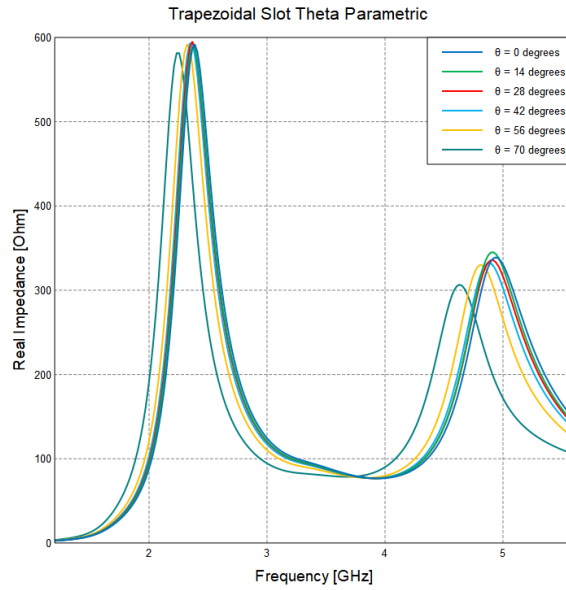
(a)
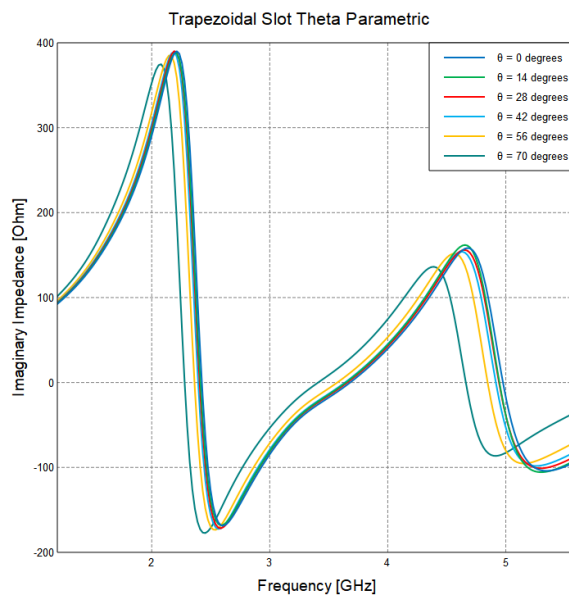
(b)

Figure 28: (a) Real impedance for the trapezoidal slot θ parametric with a small feed offset. (b) Imaginary impedance for the trapezoidal slot θ parametric with a small feed offset.

observation is expected as it matches the result of the feed offset parametric from Chapter 2. These peaks also shift with the resonances seen in the plot of the imaginary impedance. We can also see in the plot of S_{11} in Figure 29 that while the center frequency and matched region are decreasing as θ increases, the bandwidth is slightly increasing, and because of this, the FBW is found to
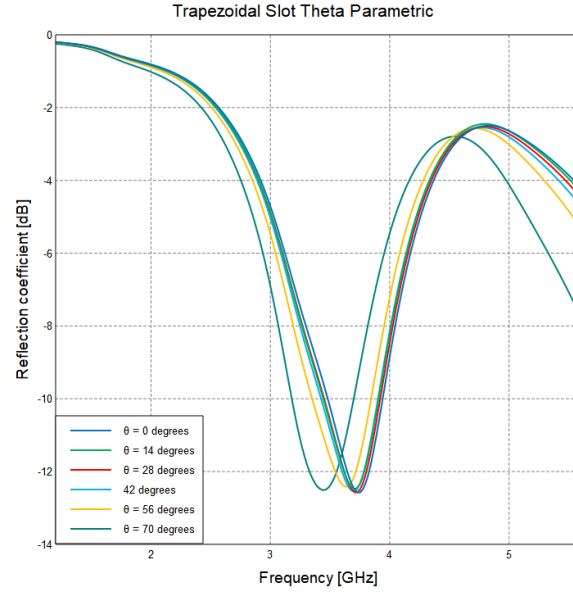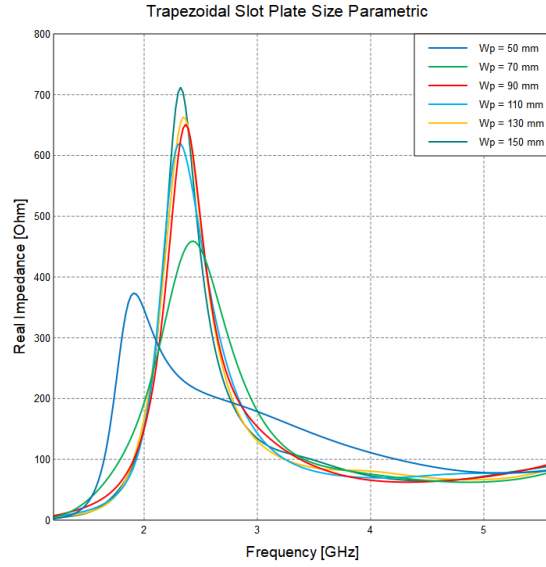
Figure 29: S$_{11}$ for the trapezoidal slot θ parametric with a small feed offset

**Table 4**: List of matched region values for the trapezoidal slot for varying θ

Theta (degrees)	Center Frequency (GHz)	Bandwidth (MHz)	FBW (%)
0	3.75	460	12.3
14	3.71	463	12.5
28	3.72	470	12.6
42	3.70	477	12.9
56	3.64	494	13.6
70	3.45	519	15.0

increase as θ increases. Table 4 lists the center frequency, bandwidth, and FBW for this parametric simulation.

While the increasing FBW matches the result found in the study of the slanted slot, the discrepancy lies in the fact the center frequency is decreasing. While for the slanted slot it was found that the center frequency corresponds to the length of the shorter side, the center frequency for the trapezoidal slot corresponds to the length of the longer side. One potential way to explain this result is because the end of an edge slot is an opening while the ends of the trapezoidal slot are the metal. When the edge slot opens at the edge of the plate, there is nothing physically present to define the end of the slot. This means that when the shorter side of the slanted slot hits the opening, there is nothing to contain the fields within the slot, which effectively ends the slot at the shorter side length even though there will be some fringing fields due to the longer side. This is

37

(a)
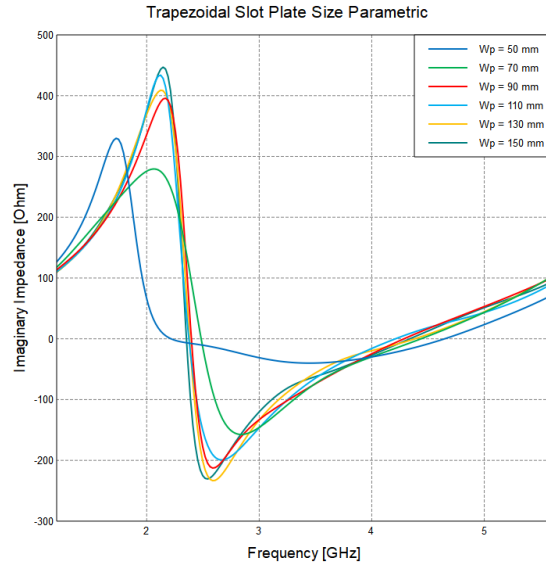
(b)

Figure 30: (a) Real impedance for the trapezoidal slot for the plate size parametric.
(b) Imaginary impedance for the trapezoidal slot for the plate size parametric.

different from a trapezoidal slot because when the ends are defined by the metal, the longer ends can be realized as an equal part of the slot.

The next parametric study done was on the plate size. The dimensions used for this study were $L_s = 51$ mm, $W_s = 3.13$ mm, $F = 0$ mm, $\theta = 45°$, W_p was varied from 50 mm to 150 mm, and L_p was adjusted to keep the ratio of $L_p/W_p = 1.15$. The dimensions L_s, W_s, and F were chosen to be the same as the plate size parametric done on the rectangular half-wave slot in Chapter 2 so that the effect from theta in the two studies could be more directly compared. The resulting impedance

simulations are shown in Figure 30. From the impedance plots it is seen that, as expected, the behavior of the slot is inhibited for small plate sizes, but once the plate width becomes greater than about 80 mm, the slot behaves as expected. The result of this simulation is similar to the simulation done on the plate size of a half-wave rectangular slot in Chapter 2.

One important difference between the slanted slot and the trapezoidal slot for the plate size parametric is that there is no notch observed from the plate resonance. The most likely reason for this is that the trapezoidal and rectangular slots are fully surrounded by large enough metallic plates that better satisfy the duality principle, which allows them to act like more ideal dipoles. Overall, these simulations on the half-wave slot show that while some of the same effects are seen for a trapezoidal slot that are seen in the slanted slot, the effects have much less of an impact on the behavior of the slot.

Chapter 5: Design Example

5.1 Problem

After the investigation of slanted slots was completed, an antenna was designed to exemplify the use of slanted slots. For this design, a center frequency, bandwidth, and maximum antenna size were specified. The design goals were to have a center frequency of 5.2 GHz, a bandwidth of at least 1.3 GHz (which is an FBW of 25%) and a maximum plate size of 7.5 cm in each dimension. The design procedure as well as the simulated and measured results for this example are given in the following sections.

5.2 Design Procedure

When designing a slanted slot, the general design procedure is as follows: calculate the length of the slot for the proper operating frequency, use Table 1 to determine θ for the desired bandwidth, and then choose initial plate size, slot width, and feed location parameters. Based on the initial results, the slot parameters can then be tuned to meet the design goals. Once these goals are met, the plate size can be reduced until the resonance frequency begins to shift away from the target frequency and the bandwidth starts to reduce. Finally, retune the slot parameters to meet the design goals again with the now smaller plate size.

The first step in the design procedure is choosing the proper slot length. Since the matched region is located at the second resonance, the slot length needs to be chosen so that it is a quarter wavelength of half the desired frequency of the matched region, which is the first resonance. For example, if the desired frequency is 4 GHz, the slot should be a quarter-wavelength long at 2 GHz. Once this slot length is determined, it should be reduced by a factor of about 0.9 due to fringing effects. This means that if the slot is ideally calculated to be 10 mm, it should be made about 9 mm long to realize the proper resonance.

The next step is to choose the proper θ for the bandwidth. This can be done by using Table 1 to see how much of a slant is necessary to realize the desired FBW. One thing to note for this step is that other slot parameters will also affect the quality of the match. This means that while Table 1 is a good reference, it will not guarantee the exact FBW specified.

After these parameters have been set, the rest of the initial parameters can be chosen. A good starting point for the width of the slot is less than about 0.03λ at the first resonance. Smaller widths will reduce the inductance and lead to a better match but would also make the slot more difficult to manufacture.

Next the dimensions of the feed need to be determined. The width of the feed should be chosen to be about the size of the center conductor in a semi-rigid coax, which is around 0.5 mm to 1 mm. In general, as the width of the feed increases, the inductance decreases. The location of the feed can also be set at around halfway along the slot. This is the feed location that will lead to a second resonance of about twice the first resonance. As the feed is moved closer to the inner edge of the slot, the real part of the impedance will decrease, the overall inductance will increase because the feed is nearing the short-circuited end, and the matched region will shift downward in frequency. As the feed is moved closer to the open edge, the opposite will happen. These trends are shown in the simulation done in Chapter 2.

Finally, the size of the plate needs to be specified. The initial choice for the plate size should be larger than at least 0.8λ at the first resonance. If there is a maximum plate size specified for the design that is close to this size, it would be suitable to use this as the initial choice. When making the choice for the plate size, one must also be cognizant of the notch frequency, which will overlap with the matched region when it is an odd-integer multiple of a half-wavelength at the second resonance. Once these parameters are all set, the rest of the procedure can be followed as described above.

5.3 Design and Simulation

Based on the study done in this thesis, it is known that for a slanted slot the bandwidth is centered around the second resonance. When the slanted slot is fed halfway between the edge of the plate and its inner edge, the first resonance will occur when the slot is approximately a quarter of a wavelength, and the second will be at approximately twice this frequency. With fringing effects causing the required length of the slot to be less exactly one-quarter of a wavelength, the initial value tried for the length of the slot was 26.7 mm. The location of the feed is also chosen to be halfway along this slot and is therefore chosen to be 13.3 mm away from the edge of the plate. To closely match the width of a semi-rigid coax feed, a tab width of 1 mm was used.

The width of the slot was initially arbitrarily chosen to be 2.5 mm since that was a common width used throughout the study. Since the slot will perform better for larger plate sizes, the original plate size tried was 75 mm by 75 mm. It is then calculated that the corresponding notch frequencies for a plate of this size will occur at around 2 GHz and 6 GHz. Since the target center frequency is 5.2 GHz, the notch frequency should not interfere with the matched region of the slot antenna. Finally, the last parameter to decide upon was θ. Based on Table 1, a θ larger than approximately 55° is required to attain an FBW of greater than 25%. Because of this, the initial value of θ used was 60°.

The result from this initial simulation was a center frequency of 5.06 GHz and an FBW of only about 20%. Since θ would need to be increased even further to improve both of these parameters but it was already fairly large, other parameters were tuned to meet the desired specifications. To increase the center frequency, the feed offset was decreased from 13.3 mm to 12.75 mm. In order to increase the FBW, the thickness of the slot was reduced to 2 mm. All other parameters were kept the same, and the slot was simulated again.

This center frequency and FBW for this simulation were 5.24 GHz and 27%, respectively. Since the FBW specification was met and the center frequency is close to the target, instead of fine-tuning any further, an attempt to reduce the plate size was undertaken. A plate size parametric from 35 mm to 75 mm was run. From this parametric, it was determined that plate sizes of 65 mm, 70 mm, and 75 mm were similar to each other while the performance of the slot began to degrade for smaller sizes. Therefore, the plate size was reduced to 65 mm by 65 mm. This plate size is only 0.56λ at the first resonance, which shows that the slot was able to be designed with a plate size smaller than the minimum 0.7λ for the rectangular edge slot.

For this configuration, however, the center frequency jumped up to 5.38 GHz. Some tuning of the feed location was performed again, and it turned out that a feed offset of 13.45 mm led to a center frequency of exactly 5.2 GHz. Unfortunately, the FBW slipped to 24.5% throughout these processes. In order to improve the FBW while preserving the center frequency, the width of the slot was further reduced to 1.5875 mm, which is one-sixteenth of an inch. Finally, for this slot configuration, the center frequency was 5.2 GHz and the bandwidth was 1.429 GHz, leading to an FBW of 27.4%. The final parameters used for this design were L_s = 26.7 mm, W_s = 1.5875 mm, F = 13.45 mm, θ = 60°, and $W_p = L_p$ = 65 mm. The resulting S_{11} plot for this antenna is shown in Figure 31.
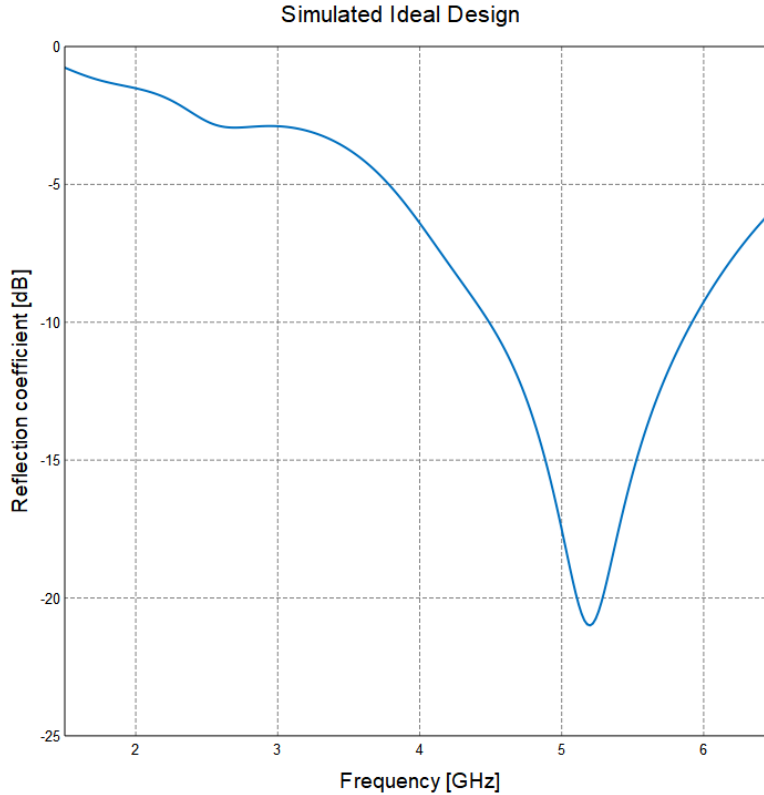
Figure 31: Simulated S_{11} for the finalized design with a center frequency of 5.2 GHz and an FBW of 27.4%

5.4 Measurements

Once the design parameters were met using simulations in FEKO©, the antenna was physically constructed. The antenna was cut out of a thin sheet of metal, and a semi-rigid coax cable was attached to the top of the plate. It was connected such that the outer conductor was soldered to the top of the plate leading up to the slot, and the inner conductor extended across the slot and was soldered to the plate on the other side of the slot. Soldering the coax to the plate in this manner has the effect of a Dyson balun [7] which allows the current on the coax to be part of the ground plane rather than producing its own radiation. The other end of the coax went to an SMA connector that hung just on the edge of the plate. The physically constructed slanted slot antenna can be seen in Figure 32. The S_{11} and radiation patterns of the antenna were also measured using a PNA and an anechoic chamber, respectively. The result from the S_{11} measurement is shown in Figure 33, and the radiation patterns measured at 5.16 GHz are shown in Figure 34.

43

Figure 32: Physically constructed slanted slot in a copper plate with a semi-rigid coax feed
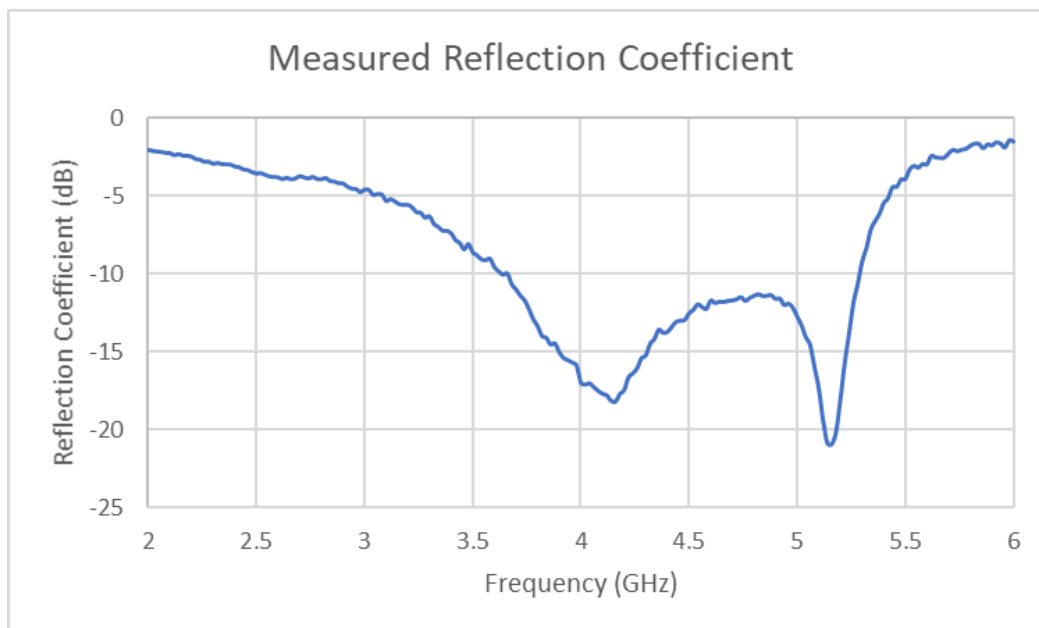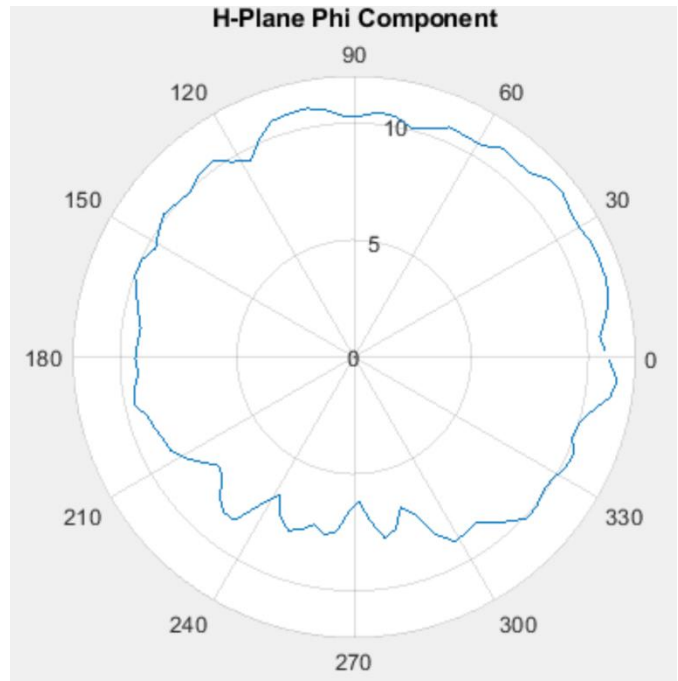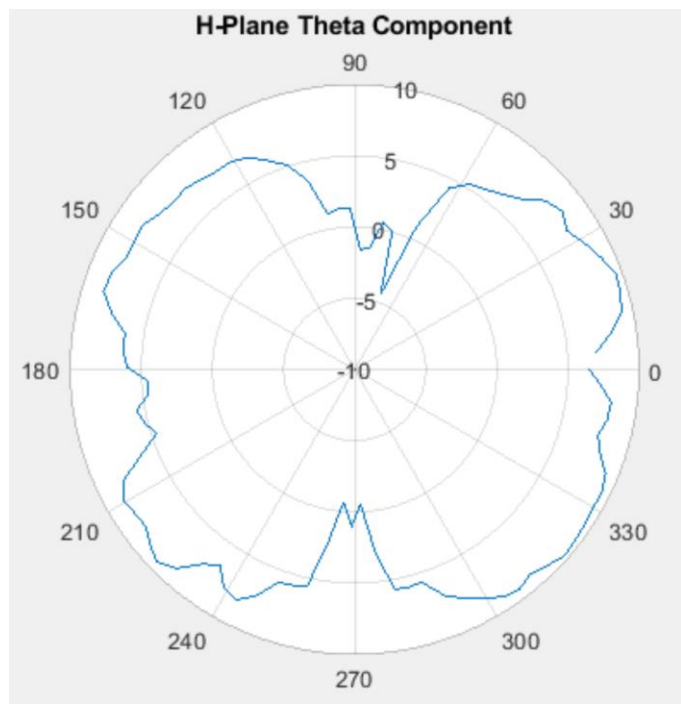

Figure 33: Measured S_{11} for the finalized design with a target center frequency of 5.2 GHz and an FBW of 27.4%
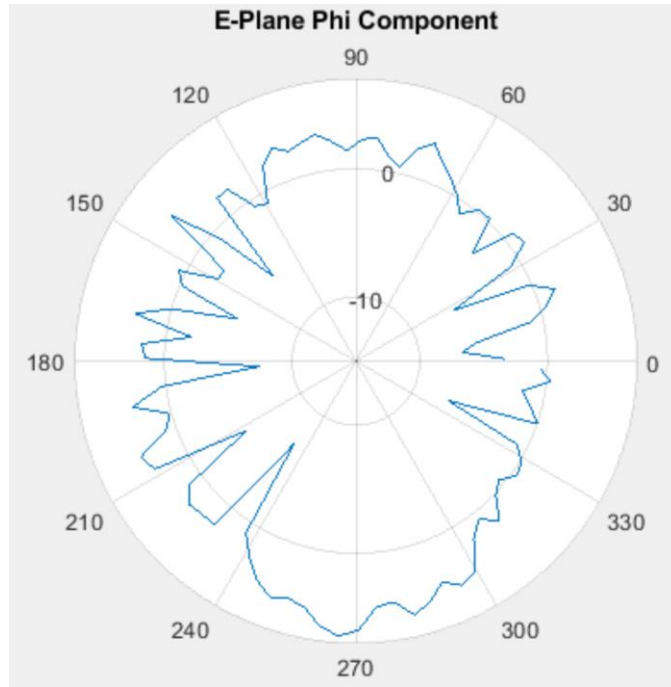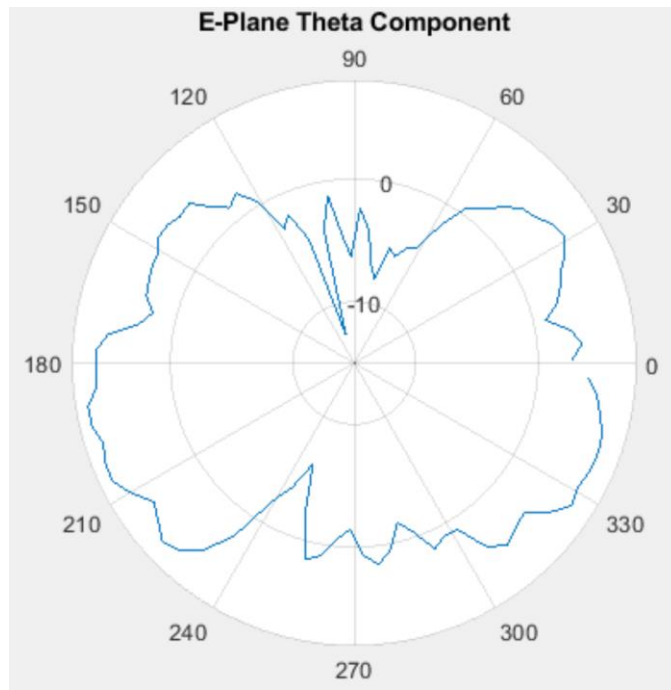
(a)

(b)

Figure 34: Far-field radiation pattern measurements for the physically constructed slanted slot antenna at 5.16 GHz (a) The H-plane Phi component. (b) The H-plane Theta component. Continued on 46.

E-Plane Phi Component

(c)

E-Plane Theta Component

(d)

Figure 34 continued. (c) The E-plane Phi component. (d) The E-plane Theta component.

From these results, it is seen that the matched region was much larger than predicted and occurs at a lower frequency. The overall center frequency was 4.46 GHz and the bandwidth was 1.64 GHz, which led to an FBW of 36.8%. This means that this antenna has met the required bandwidth, but the center frequency is incorrect. However, also from Figure 33, it appears as though the overall matched region was comprised of two separate matched regions that merged together. The first one was located at 4.16 GHz, and the second was at 5.16 GHz.

The second matched region had a slightly better match than the first, and based on its shape and frequency location, it can be attributed to the slot. The first matched region, however, was not predicted by the simulation. It occurs at a frequency of 4.16 GHz, which has a wavelength of about 72 mm. This is not near either of the two plate resonances which would occur at 130 mm or 43 mm, so the plate could not have caused this. The longer arm of the coax feed was measured at about 37 mm. This distance is nearly one half of a wavelength at 4.16 GHz. This indicates that the most likely cause of the first matched region would be from the coax. The Dyson balun should have prevented this; however, it could be that not all the soldering joints along the plate provide a solid enough contact to allow the currents to flow seamlessly across the entire coax and plate. The reason for this match could also be that at 4.16 GHz, the slot is not a good match, and the presence of the Dyson balun along with the fact that the plate is small at this frequency could cause more currents to appear on the cable.

Next, when looking at the radiation patterns plotted in MATLAB$^©$, it is seen that the measured radiation patterns generally follow the expected radiation patterns from Figure 15 in Chapter 3, but there is a lot of ringing. The Theta components were mostly omnidirectional except for being weaker in the plane of the metallic plate. The Phi component in the H-plane is more directed to the 90° half of the H-plane, which is the side of the plate with the slot opening. The Phi component in the E-plane was also larger in the direction the slot was pointing. Both results match the trends seen in the simulation in Chapter 3. While the patterns generally match the simulated results, there is a lot of ringing still seen. This is most likely from the cable, which further indicates that the coax was not thoroughly soldered down and contributed to the radiation.

Another potential cause for the measured results to deviate from the simulated results was imperfect construction of the slot. The entire slot was built and soldered by hand rather than precision tools, thereby causing the slot dimensions to deviate slightly from the ideal design. After building the slanted slot antenna, its actual dimensions were measured, and a simulation was
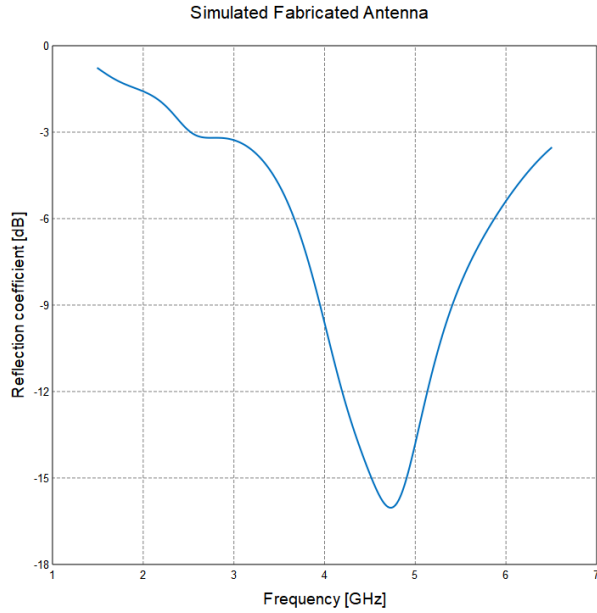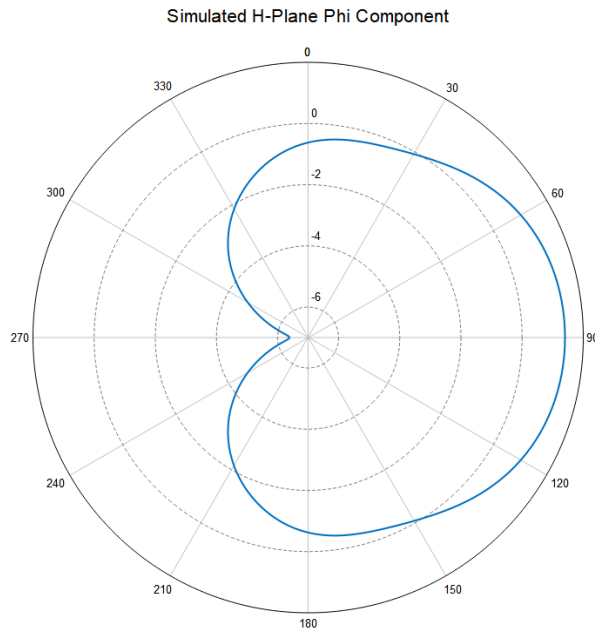
Figure 35: Simulated S_{11} for the slanted slot using the parameters measured from the physically constructed slanted slot

(a)

Figure 36: Simulated radiation patterns for the designed slanted slot using the measured parameters from the constructed slanted slot. (a) The H-plane Phi component. Continued on 49.

performed using these measured values. It was measured that $L_s = 27.05$ mm, $W_s = 1.65$, $\theta = 59.8°$, $F = 14.5$ mm, $W_p = 65.15$ mm, and $L_p = 65.4$ mm. The simulated S_{11} and radiation patterns are shown in Figures 35 and 36, respectively.
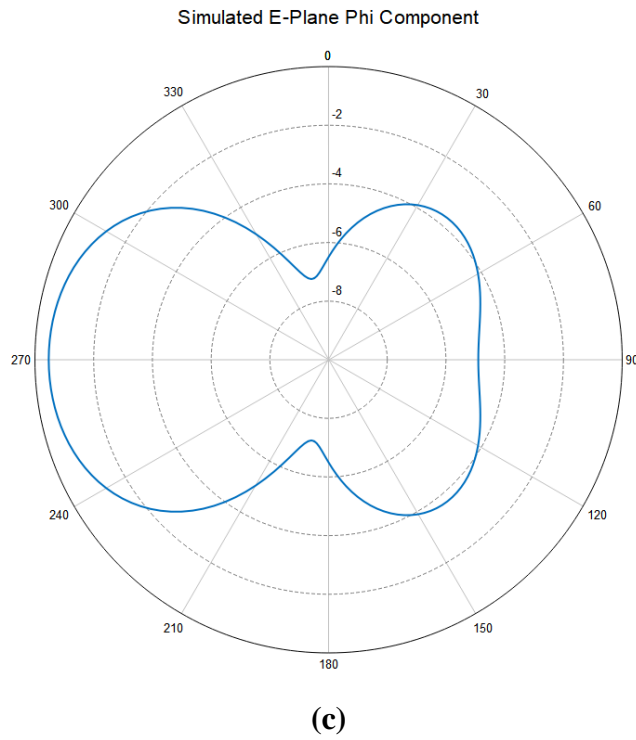
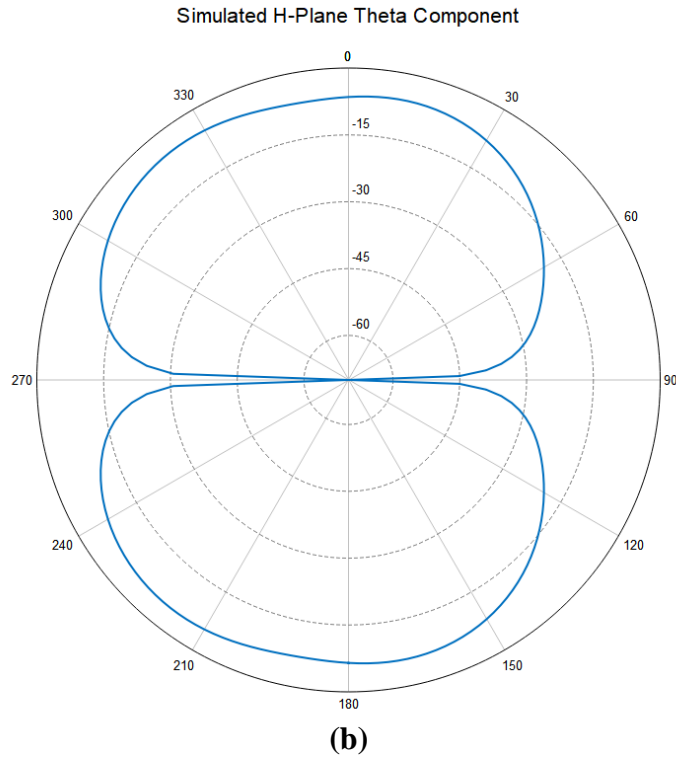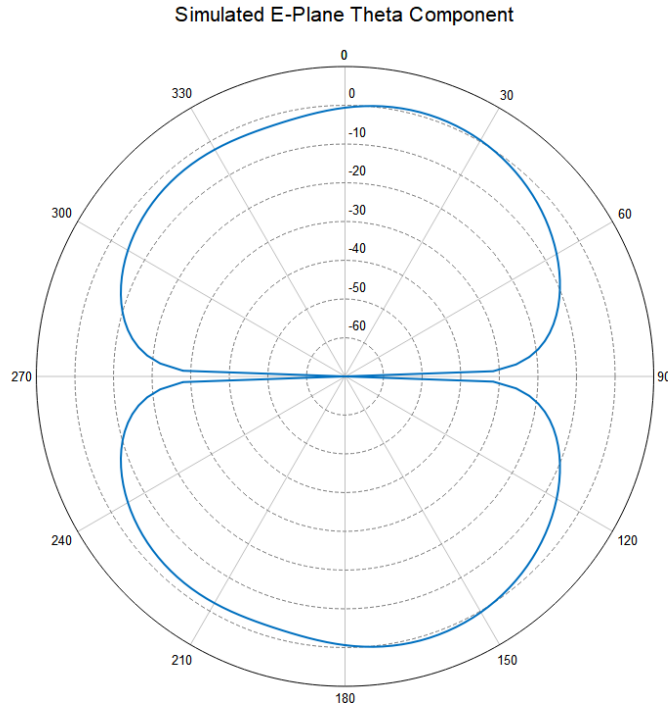48

(b)

(c)

Figure 36 continued. (b) The H-plane Theta component. (c) The E-plane Phi component. Continued on 50.

49

Simulated E-Plane Theta Component

(d)

Figure 36 continued. (d) The E-plane Theta component.

It is seen from these figures that the operating frequency of the slot should have been closer to 4.74 GHz rather than 5.2 GHz. This large discrepancy is due to the fact that both the slot was longer and the feed offset was larger than they were designed to be. While these discrepancies affected the S_{11} of the antenna, the radiation pattern remained similar to what was expected from the study done in Chapter 3 and what was observed with the measurements. One important note for the plots of the radiation patterns is that the plots output from FEKO© have Theta equal to zero at the top and 90° to the right, whereas the plots produced by MATLAB© have Theta equal to zero to the right and 90° at the top.

Chapter 6: Conclusion

Through this study of the slanted slot, it was found that the bandwidth of a quarter-wave slot antenna can be increased by placing the slot on an angle coming off the edge of a metallic plate. The fractional bandwidth was about 1.5 times larger for a slot on a 60° angle than for one perpendicular to the edge. This study also showed that the plate size has a significant impact on the behavior of the antenna; however, putting the slot on a slant made its behavior more robust to changes in the plate size. When the same study was performed on an analogous trapezoidal slot, similar results were attained in that the fractional bandwidth was successfully increased, but the increase was less substantial than that with the slanted slot. It was also found that the plate size for the rectangular and trapezoidal slots had little impact on the slot behavior and could be reasonably ignored once the plate became larger than approximately 0.8λ. Overall, these results show that a slanted slot is able to provide a small, reliable, and easy-to-manufacture antenna while also achieving a larger more consistent bandwidth than for a regular quarter-wave edge slot.

These results are promising, and there is room for future work. One area of future work would be to add a dielectric and a separate ground plane. Another area for future work would be to make these slots tunable using a tuning element. Characteristic mode and transmission line studies of these slanted slots would also be beneficial to observe more of the underlying impact of changing the side lengths of a slot or putting it on a slant. Finally, another area of future work could be placing multiple slanted slots on the same plate. While there is still more to explore with slanted slots, this thesis shows that they can be used to enhance the bandwidth of an edge slot antenna and make it more robust to changing plate sizes.

References

[1] J. Wu, C. Lin, and J. Lu, "A planar meander-line antenna for triple-band operation of mobile handsets," *Microw. Opt. Technol. Lett.*, vol. 41, pp. 380-386, 2004.

[2] D. Yu, W. L. Liu and Z. H. Zhang, "Simple structure multiband patch antenna with three slots," *2012 International Conference on Microwave and Millimeter Wave Technology (ICMMT)*, Shenzhen, 2012, pp. 1-3.

[3] S. Weigand, G. H. Huff, K. H. Pan and J. T. Bernhard, "Analysis and design of broad-band single-layer rectangular U-slot microstrip patch antennas," *IEEE Transactions on Antennas and Propagation*, vol. 51, no. 3, pp. 457-468, March 2003.

[4] A. Sajee, "Broadband design and simulation of trapezoidal slot of microstrip antenna," *ARPN Journal of Engineering and Applied Sciences*, vol. 7, pp. 127-135, 2012.

[5] G.V. Raviteja, "Design and analysis of a novel dual trapezoidal slot-based rectangular microstrip antenna for wide area network using WiMax application," *Microw Opt Technol Lett*, vol. 60, pp. 1057– 1060, 2018.

[6] J. D. Kraus and R. J. Marhefka, *Antennas For All Applications*, 3rd ed. New York City, NY: McGraw-Hill Companies, Inc., 2002.

[7] J. Dyson, "The unidirectional equiangular spiral antenna," *IRE Transactions on Antennas and Propagation*, vol. 7, no. 4, pp. 329-334, October 1959.